Table 2
Intracellular distribution of electron-dense particles with an approximate diameter of 55 nm at 4 h post-inoculation.

	Number of 55-nm electron-dense particles[a]									
	Cell surface		LBs		MVBs		L-MVBs		Cytosol	
	#1	#2	#1	#2	#1	#2	#1	#2	#1	#2
16PV	27	140	2.5	0.4	13	19	12	15	1.8	1.4
16PV + anti-P56/75	28	110	0	0	7	1.4	4.3	0.8	0	0

Experiments were performed twice independently.
[a] The number of particles is shown as the average from five cells photographed at a magnification of ×20,000.

both the presence and absence of antibody, 16PV particles were observed on the surface of inoculated HeLa cells. Thus, anti-P56/75 did not neutralize 16PV by interfering with viral attachment to cells.

The binding of anti-P56/75 to 16PV partially blocked the entry of cell-attached 16PV into HeLa cells. After incubation of inoculated HeLa cells at 37 °C, the trypsin resistance of the L1 protein of antibody-bound 16PV was only 80% of the trypsin resistance of 16PV L1 in the absence of antibody, indicating that 20% of antibody-bound 16PV remained on the cell surface, where it appeared to form aggregates visible by confocal microscopy after 2 to 22 h of incubation. The aggregates were also observed by electron microscopy, suggesting that the aggregates that formed after the attachment of PV to the surface were not degraded and remained for a long period on the cell surface. This indicates that anti-P56/75 did not mediate the formation of large aggregates of virion by acting as a bivalent tether. In a similar previous experiment, 16PV bound with RG-1, a monoclonal antibody recognizing amino acids 17–36 of L2, accumulated in the extracellular matrix contacting the cell edges (Day et al., 2008).

The binding of anti-P56/75 to 16PV blocked the release of the packaged DNA from the internalized PV to the nucleus. On confocal fluorescence micrographs, DNA released from capsids was observed in the nuclei of cells inoculated with 16PV preincubated with normal serum and incubated for 22 h; however, no evidence of released DNA was seen in cells inoculated with antibody-bound 16PV.

Electron micrographs of HeLa cells at 4 h after the inoculation clearly showed that cells inoculated with antibody-bound 16PV contained fewer 16PV particles than cells inoculated with 16PV in the absence of antibody, even though the antibody impaired the internalization efficiency of 16PV by only about 20%. It is possible that the capsids of antibody-bound 16PV were easily denatured in the cells, making some particles undetectable by electron microscopy. Based on the electron micrographs, antibody-bound 16PV entered the cells by endocytosis, but failed to egress from endosomal vesicles. In the absence of antibody, 16PV particles were seen in MVBs, LBs, and the cytosol (Fig. 4C), whereas particles of antibody-bound 16PV were observed in some MVBs, but not in the cytosol. Previous studies have shown that the most BPV1 virions, BPV1 PV, HPV16 capsids, and HPV31 capsids accumulate in endosomal vesicles (Zhou et al., 1995; Bossis et al., 2005; Bousarghin et al., 2003), and a small fraction of inoculated HPV16 capsids or BPV1 PV has been detected in the cytosol (Yang et al., 2003; Bossis et al., 2005). In general, particles in endosomal vesicles are degraded after fusion of the vesicles with lysosomes (Day et al., 2003). In the present study, the particles observed in the cytosol might have been those that escaped degradation.

The structure of particles in the cytosol must be altered in order to release the viral genome from the virion. These dynamic structural changes may be induced by cyclophilin A, a cytosolic peptidyl-prolyl cis/trans isomerase that facilitates 16PV infection (Bienkowska-Haba et al., 2009), and by cell cycle progression through mitosis, which is an important event for HPV infection (Pyeon et al., 2009).

The attachment of particles to the limiting membranes of MVBs, as reported in the present study, may be vital for particles to exit the vesicles, considering that no antibody-bound 16PV particles were found attached to MVB limiting membranes or in the cytosol. A previous study suggested that HPV L2 bound to the lipid bilayer of endosomal compartments and destabilized the membrane, according to a decrease of the internal pH (Kämper et al., 2006); this eventually led to the viral genome entering the nucleus. Anti-P56/75 binds to the L2 region displayed on the surface of HPV pseudovirus (Kondo et al., 2007) and may thereby block an L2 function necessary for binding to and destabilizing the limiting membrane.

In summary, 16PV alone and antibody-bound 16PV showed similar attachment to the surface of HeLa cells. Almost all of the cell-attached 16PV and approximately 80% of the cell-attached antibody-bound 16PV entered cells by endocytosis after incubation at 37 °C. Approximately 20% of the cell-attached antibody-bound particles remained on the surface, where they formed aggregates. A portion of the 16PV particles exited the vesicles and transported the packaged DNA to the nucleus. In contrast, all of the antibody-bound 16PV particles remained in vesicles, to be degraded after the fusion of the vesicles with lysosomes. It is likely that an L2 function essential for egress from vesicles is abrogated by the binding of anti-P56/75 antibody. This study suggests that anti-P56/75 inhibits HPV infection partly by blocking viral entry and primarily by blocking the transport of the viral genome to the nucleus.

Materials and methods

Cells

The 293FT cell line expressing a high level of SV40 T-antigen was purchased from Life Technologies Corp. (Carlsbad, CA, USA). The 293FT and HeLa cells were cultured in Dulbecco's modified Eagle's medium (DMEM) (Life Technologies Corp.) supplemented with 10% fetal bovine serum, 100 units/ml penicillin G potassium (Meiji Seika Ltd., Tokyo, Japan), and 60 μg/ml kanamycin sulfate (Wako Pure Chemical Industries Ltd., Tokyo, Japan) at 37 °C in 5% CO_2.

Production of 16PV

The 16PV consisted of a HPV16 capsid containing a reporter plasmid encoding enhanced green fluorescence protein (pEF1a-EGFP) and was produced as described previously (Ishii et al., 2007; Kondo et al., 2007). To label the 16PV-packaged DNA with 5-ethynil-2′-deoxyuridine (EdU) (Life Technologies Corp.), 293FT cells (1×10^7) were incubated for 16 h in a 10-cm culture dish; transfected with a mixture of p16L1h (13.5 μg), p16L2h (3 μg), and pYSEAP (13.5 μg) (Kondo et al., 2007) by using Fugene HD (Roche Diagnostics GmbH, Mannheim, Germany); incubated for 6 h at 37 °C; and supplemented with 100 μM EdU. After 60 h, the cells were harvested using a cell scraper, suspended in 500 μl of lysis buffer [PBS containing 1 mM $CaCl_2$, 10 mM $MgCl_2$, 0.35% Brij58 (Sigma-Aldrich, St. Louis, MO, USA), 0.1% benzonase (Sigma-Aldrich), 0.1% plasmid-safe ATP-dependent DNase (Epicentre Corp., Madison, WI, USA), and 1 mM ATP], and incubated for 30 h at 37 °C with slow rotation, in the dark. The lysate was cooled on ice for 5 min, mixed with 5 M NaCl to a final NaCl concentration of 1 M, kept on ice for 10 min, and then centrifuged at 5000×*g* for 10 min at 4 °C. The supernatant was placed on an Optiprep (Axis-Shield PoC AS, Oslo, Norway) gradient (from top to bottom, 27%, 33%, and 39% in PBS containing 1 mM $CaCl_2$, 10 mM $MgCl_2$, and 0.85 M NaCl) and centrifuged at 50,000 rpm for 3.5 h at 16 °C in an SW55Ti rotor (Beckman Coulter Inc., Fullerton, CA, USA). Fractions (400 μl each) were obtained by puncturing the bottom of the tube. Aliquots (5 μl per fraction) were analyzed by SDS-PAGE. The fraction in which L1 was most abundant was used as the 16PV stock.

Neutralization assay

The 16PV (0.25 μg or 2.5 μg of L1) was mixed with normal rabbit serum (Life Technologies Corp.) or rabbit anti-P56/75 serum (Kondo et al., 2007), at serial dilutions from 1:20 to 1:800, in 500 μl of growth medium and incubated at 37 °C for 30 min. Each mixture was added to HeLa cells (1.5×10^5) in 24-well plates. After incubation for 2 days, the cells were examined under a BZ-8000 fluorescence microscope (Keyence, Osaka, Japan) and harvested using trypsin. EGFP-positive cells were counted by flow cytometry (FACSCalibur; Becton Dickinson and Co., San Jose, CA, USA).

Western blot assay

The 16PV (2.5 μg of L1) was mixed with normal rabbit serum or rabbit anti-P56/75 serum (1:20 dilution) in 500 μl of growth medium and incubated at 37 °C for 30 min. Each mixture was added to HeLa cells (1.5×10^5) in 24-well plates. The cells were incubated for 1 h at 4 °C, washed with PBS, harvested in PBS containing 2.5 mM EDTA, and lysed. The lysate proteins were separated by SDS-PAGE and transferred to a polyvinylidene difluoride membrane. The L1 protein was detected by immunoblotting with mouse monoclonal anti-HPV16 L1 antibody (BD Biosciences Pharmingen, San Diego, CA, USA), followed by anti-mouse IgG-HRP (Santa Cruz Biotechnology Inc., Santa Cruz, CA, USA). Immunoreactive bands were visualized using an ECL Plus Western blot detection system (GE Healthcare UK Ltd., Little Chalfont, Buckinghamshire, England) and Typhoon 9410 (GE Healthcare UK Ltd.).

Internalization assay

The 16PV (2.5 μg of L1) was mixed with normal rabbit serum or rabbit anti-P56/75 serum (1:20 dilution) in 500 μl of growth medium and incubated at 37 °C for 30 min. Each mixture was added to HeLa cells (1.5×10^5) in 24-well plates. After incubation for 1 h at 4 °C, the cells were washed with PBS, cultured at 37 °C for 0, 2, 4, 8, and 22 h, and harvested with PBS containing trypsin (trypsin+) or containing 2.5 mM EDTA (trypsin−). The cells were lysed and electrophoresed in a SDS-polyacrylamide gel. The separated proteins were transferred to a polyvinylidene difluoride membrane, and a Western blot was performed as described above.

Immunofluorescence assay

The 16PV (2.5 μg of L1) containing EdU-labeled DNA was mixed with normal rabbit serum or rabbit anti-P56/75 serum (1:20 dilution) in 500 μl of growth medium and incubated at 37 °C for 30 min. The mixture was added to HeLa cells (1.5×10^5) in the wells of four-chamber glass slides (BD Biosciences Falcon, Bedford, MA, USA), followed by incubation for 1 h at 4 °C. The cells were washed with growth medium, incubated in growth medium for 0, 2, 4, 8, and 22 h at 37 °C, washed with PBS, and fixed with methanol for 30 min at −20 °C. After washing twice with 3% BSA in PBS for 5 min, the cells were incubated with Click-it Reaction Cocktail containing Alexa Fluor 488 (Click-it™ EdU imaging kit; Life Technologies Corp.) for 30 min at room temperature (RT) in the dark and again washed twice with 3% BSA in PBS for 5 min. Next, the cells were incubated with mouse anti-HPV16 L1 polyclonal antiserum, which had been produced previously by immunizing mice with HPV16 L1 VLP (Ishii et al., 2003), in PBS containing 3% BSA for 1 h at RT and washed with PBS containing 0.2% Tween-20. The cells were then incubated with Alexa Fluor 555-conjugated goat anti-mouse IgG (H+L) (Life Technologies Corp.) in PBS containing 3% BSA, washed with PBS containing 0.2% Tween-20, and mounted with ProLong Gold anti-fade reagent with DAPI (Life Technologies Corp.). Fluorescence was examined using a Fluoview FV1000 confocal microscope (Olympus, Tokyo, Japan).

Electron microscopy

The 16PV (10 μg of L1) was mixed with normal rabbit serum or rabbit anti-P56/75 serum (1:10 dilution) in 1 ml of growth medium and incubated at 37 °C for 30 min. Each mixture was added to HeLa cells (6×10^5) in 35-mm culture plates. After incubation at 37 °C for 1 h, 1 ml of growth medium was added to the cells, and the cells were incubated at 37 °C for another 3 h (4 h total). After incubation, the cells were prefixed in 2.5% glutaraldehyde/0.1 M phosphate buffer at RT for 2 h, washed with phosphate buffer for 30 min, and post-fixed in 1% osmium tetroxide for 1 h. Following dehydration in a graded series of ethanol solutions, the cells were embedded in a mixture of Epoxy 812, DDSA, MNA, and DMP-30 at 60 °C for 2 days. Ultra-thin sections (70 nm) were cut parallel to the substrate, stained with 4% uranyl acetate, and examined under a Hitachi H-7650 transmission electron microscope.

Acknowledgments

This work was supported by a grant-in-aid for the Third-Term Comprehensive 10-year Strategy for Cancer Control from the Ministry of Health, Labour, and Welfare of Japan.

Appendix A. Supplementary data

Supplementary data associated with this article can be found, in the online version, at doi:10.1016/j.virol.2010.07.019.

References

Bienkowska-Haba, M., Patel, H.D., Sapp, M., 2009. Target cell cyclophilins facilitate human papillomavirus type 16 infection. PLoS Pathog. 5, e1000524.
Bossis, I., Roden, R.B., Gambhira, R., Yang, R., Tagaya, M., Howley, P.M., Meneses, P.I., 2005. Interaction of tSNARE syntaxin 18 with the papillomavirus minor capsid protein mediates infection. J. Virol. 79, 6723–6731.
Bousarghin, L., Touzé, A., Sizaret, P.Y., Coursaget, P., 2003. Human papillomavirus types 16, 31, and 58 use different endocytosis pathways to enter cells. J. Virol. 77, 3846–3850.
Buck, C.B., Pastrana, D.V., Lowy, D.R., Schiller, J.T., 2004. Efficient intracellular assembly of papillomaviral vectors. J. Virol. 78, 751–757.
Conway, M.J., Alam, S., Christensen, N.D., Meyers, C., 2009. Overlapping and independent structural roles for human papillomavirus type 16L2 conserved cysteines. Virology 393, 295–303.
Day, P.M., Lowy, D.R., Schiller, J.T., 2003. Papillomaviruses infect cells via a clathrin-dependent pathway. Virology 307, 1–11.
Day, P.M., Baker, C.C., Lowy, D.R., Schiller, J.T., 2004. Establishment of papillomavirus infection is enhanced by promyelocytic leukemia protein (PML) expression. Proc. Natl. Acad. Sci. U.S.A. 101, 14252–14257.
Day, P.M., Gambhira, R., Roden, R.B., Lowy, D.R., Schiller, J.T., 2008. Mechanisms of human papillomavirus type 16 neutralization by L2 cross-neutralizing and L1 type-specific antibodies. J. Virol. 82, 4638–4646.
Finnen, R.L., Erickson, K.D., Chen, X.S., Garcea, R.L., 2003. Interactions between papillomavirus L1 and L2 capsid proteins. J. Virol. 77, 4818–4826.
Giroglou, T., Florin, L., Schäfer, F., Streeck, R.E., Sapp, M., 2001. Human papillomavirus infection requires cell surface heparan sulfate. J. Virol. 75, 1565–1570.
Hindmarsh, P.L., Laimins, L.A., 2007. Mechanisms regulating expression of the HPV 31 L1 and L2 capsid proteins and pseudovirion entry. Virol. J. 4, e19.
Howley, P.M., Lowy, D.R., 2001. Papillomaviruses and their replication, In: Lnipe, D.M., Howley, P.M. (Eds.), 4th ed. Fields Virology, Vol 2. Lippincott, Williams&Wilkins, Philadelphia, pp. 2197–2229.
Ishii, Y., Tanaka, K., Kanda, T., 2003. Mutational analysis of human papillomavirus type 16 major capsid protein L1: the cysteines affecting the intermolecular bonding and structure of L1-capsids. Virology 308, 128–136.
Ishii, Y., Kondo, K., Matsumoto, T., Tanaka, K., Shinkai-Ouchi, F., Hagiwara, K., Kanda, T., 2007. Thiol-reactive reagents inhibits intracellular trafficking of human papillomavirus type 16 pseudovirions by binding to cysteine residues of major capsid protein L1. Virol. J. 4, 110.
Kämper, N., Day, P.M., Nowak, T., Selinka, H.C., Florin, L., Bolscher, J., Hilbig, L., Schiller, J. T., Sapp, M., 2006. A membrane-destabilizing peptide in capsid protein L2 is required for egress of papillomavirus genomes from endosomes. J. Virol. 80, 759–768.
Kondo, K., Ishii, Y., Ochi, H., Matsumoto, T., Yoshikawa, H., Kanda, T., 2007. Neutralization of HPV16, 18, 31, and 58 pseudovirions with antisera induced by immunizing rabbits with synthetic peptides representing segments of the HPV16 minor capsid protein L2 surface region. Viroloy 358, 266–272.

Okun, M.M., Day, P.M., Greenstone, H.L., Booy, F.P., Lowy, D.R., Schiller, J.T., Roden, R.B., 2001. L1 interaction domains of papillomavirus L2 necessary for viral genome encapsidation. J. Virol. 75, 4332–4342.

Pastrana, D.V., Gambhira, R., Buck, C.B., Pang, Y.Y., Thompson, C.D., Culp, T.D., Christensen, N.D., Lowy, D.R., Schiller, J.T., Roden, R.B., 2005. Cross-neutralization of cutaneous and mucosal Papillomavirus types with anti-sera to the amino terminus of L2. Virology 337, 365–372.

Pyeon, D., Pearce, S.M., Lank, S.M., Ahlquist, P., Lambert, P.F., 2009. Establishment of human papillomavirus infection requires cell cycle progression. PLoS Pathog. 5, e1000318.

Richards, R.M., Lowy, D.R., Schiller, J.T., Day, P.M., 2006. Cleavage of the papillomavirus minor capsid protein, L2, at a furin consensus site is necessary for infection. Proc. Natl. Acad. Sci. U.S.A. 103, 1522–1527.

Schmitz, G., Müller, G., 1991. Structure and function of lamellar bodies, lipid–protein complexes involved in storage and secretion of cellular lipids. J. Lipid Res. 32, 1539–1570.

Smith, J.L., Campos, S.K., Wandinger-Ness, A., Ozbun, M.A., 2008. Caveolin-1-dependent infectious entry of human papillomavirus type 31 in human keratinocytes proceeds to the endosomal pathway for pH-dependent uncoating. J. Virol. 82, 9505–9512.

Spoden, G., Freitag, K., Husmann, M., Boller, K., Sapp, M., Lambert, C., Florin, L., 2008. Clathrin- and caveolin-independent entry of human papillomavirus type 16-involvement of tetraspanin-enriched microdomains (TEMs). PLoS ONE 3, e3313.

Yang, R., Yutzy 4th, W.H., Viscidi, R.P., Roden, R.B., 2003. Interaction of L2 with beta-actin directs intracellular transport of papillomavirus and infection. J. Biol. Chem. 278, 12546–12553.

Zhou, J., Gissmann, L., Zentgraf, H., Müller, H., Picken, M., Müller, M., 1995. Early phase in the infection of cultured cells with papillomavirus virions. Virology 214, 167–176.

zur Hausen, H., 2002. Papillomaviruses and cancer: from basic studies to clinical application. Nat. Rev. Cancer 2, 342–350.

Biased amplification of human papillomavirus DNA in specimens containing multiple human papillomavirus types by PCR with consensus primers

Seiichiro Mori,[1,4,5] Sari Nakao,[1,5] Iwao Kukimoto,[1] Rika Kusumoto-Matsuo,[1] Kazunari Kondo[2] and Tadahito Kanda[1,3]

[1]Pathogen Genomics Center, National Institute of Infectious Diseases, Shinjuku-ku, Tokyo; [2]NTT Medical Center Tokyo, Shinagawa-ku, Tokyo; [3]Center of Research Network for Infectious Diseases, Riken, Chiyoda-ku, Tokyo, Japan

(Received January 18, 2011/Revised March 2, 2011/Accepted March 2, 2011/Accepted manuscript online March 9, 2011)

Genotyping human papillomavirus (HPV) in clinical specimens is important because each HPV type has different oncogenic potential. Amplification of HPV DNA by PCR with the consensus primers that are derived from the consensus sequences of the *L1* gene has been used widely for the genotyping. As recent studies have shown that the cervical specimens often contain HPV of multiple types, it is necessary to confirm whether the PCR with the consensus primers amplifies multiple types of HPV DNA without bias. We amplified HPV DNA in the test samples by PCR with three commonly used consensus primer pairs (L1C1/L1C2+C2M, MY09/11, and GP5+/6+), and the resultant amplicons were identified by hybridization with type-specific probes on a nylon membrane. L1C1/L1C2+C2M showed a higher sensitivity than the other primers, as defined by the ability to detect HPV DNA, on test samples containing serially diluted one of HPV16, 18, 51, 52, and 58 plasmids. L1C1/L1C2+C2M failed to amplify HPV16 in the mixed test samples containing HPV16, and either 18 or 51. The three consensus primers frequently caused incorrect genotyping in the selected clinical specimens containing HPV16 and one or two of HPV18, 31, 51, 52, and 58. The data indicate that PCR with consensus primers is not suitable for genotyping HPV in specimens containing multiple HPV types, and suggest that the genotyping data obtained by such a method should be carefully interpreted. (*Cancer Sci*, doi: 10.1111/j.1349-7006.2011.01922.x, 2011)

Human papillomavirus (HPV), composed of an icosahedral capsid and a circular double-stranded DNA genome, is classified into more than 100 genotypes based on the nucleotide sequence homology of the *L1* gene encoding the major capsid protein.[1] The HPV types found in lesions of the skin and genital mucosa are grouped as cutaneous and genital HPVs, respectively. Of genital HPVs, 15 types (HPV16, 18, 31, 33, 35, 39, 45, 51, 52, 56, 58, 59, 66, 68, and 73) that have been found in cervical cancer are called high-risk HPVs[2] and the types, such as HPV6 and HPV11, that have been found in benign genital warts are called low-risk HPVs.[3]

For detection and genotyping of HPV DNA in the clinical specimens, such as cervical swabs and Pap smears, a part of the *L1* gene is amplified by PCR then grouped based on the susceptibility to various restriction enzymes, the binding capacity to type-specific probes, or the nucleotide sequences of the amplicons.[4] Several consensus primer pairs have been developed and used as standard primers for PCR-based genotyping of HPV in the clinical specimens. L1C1/L1C2+C2M was developed in 1991,[5] and has been used in more than 10 articles describing HPV prevalence in the Japanese population.[5–16] MY09/11[17] and GP5+/6+[18] were developed in 1989 and 1995, respectively, and have been used in numerous studies worldwide.[19] These primers are derived from the consensus sequences of the *L1* gene and the amplicons contain type-specific sequences. Recently new primers, PGMY09/11[20] and modified GP5+/6+ (MGP),[21] which are composed of several type-specific primers, were developed to improve the accuracy of HPV genotyping. The World Health Organization HPV Laboratory Network, which was founded to improve the quality of laboratory services for effective surveillance and monitoring of HPV vaccination impact, recommends PCR with PGMY09/11 followed by reverse blotting hybridization with type-specific probes, as a standard procedure for HPV genotyping.[22]

Recent studies showed that many HPV-positive women are infected with multiple genotypes.[23,24] Therefore, the methods capable of detecting and genotyping HPV DNA of multiple types in a single clinical specimen are necessary to know the precise prevalence of HPV types and the impact of HPV vaccines. As PCR does not always amplify different DNA fragments with equal efficiency, we examined whether PCR with consensus primers can amplify HPV DNA of multiple genotypes in a single sample without bias. We found that PCR with consensus primers sometimes results in mistyping.

Materials and Methods

Plasmids. The pUC plasmid containing the complete genome of HPV16, 18, 31, 51, or 52, or the *L1* gene of HPV58 was used. Purified plasmids were quantified with the NanoDrop ND-1000 (Thermo Fisher Scientific, Waltham, MA, USA). The copy numbers of HPV genomes were calculated from the concentration of plasmid expressed as molarities and Avogadro's number.

Clinical specimens. Cervical exfoliated cells were collected from outpatients who visited the NTT Medical Center Tokyo, with their informed consent. The study design and sample collection were approved by the institutional review board. One case of normal cytology, two cases of cervical intraepithelial neoplasia (CIN) grade 1, two cases of CIN2, two cases of CIN3, and one case of unknown cytology were selected for this study. DNA was purified using the QIAamp DNA blood kit (Qiagen, Hilden, Germany).

Polymerase chain reaction. Table 1 shows the sequences of primers used in this study: three consensus primer pairs, L1C1/L1C2+C2M,[5] MY09/11,[17] and GP5+/6+;[18] and two mixtures of type-specific primers, PGMY09/11[20] and modified GP5+/6+ (MGP).[21] Polymerase chain reaction amplification was done in a 50 μL reaction mixture containing 1× PCR buffer II (Life Technologies, Carlsbad, CA, USA), 1.25 units AmpliTaq Gold DNA polymerase (Life Technologies), and 50 ng cellular DNA extracted from human HaCaT cells. The 5′-end of either the forward or reverse primer was biotinylated. The concentrations of MgCl2, dNTPs, and primers, and the reaction temperature were adjusted to those used in the original article

[4]To whom correspondence should be addressed. E-mail: moris@nih.go.jp
[5]These authors contributed equally to this work.

doi: 10.1111/j.1349-7006.2011.01922.x

Table 1. Nucleotide sequences of primers used in this study

	Primer set	Forward (5′–3′)	Reverse (5′–3′)
Consensus primers	L1C1/L1C2+C2M	CGTAAACGTTTTCCCTATTTTTTT	TACCCTAAATACTCTGTATTG
			TACCCTAAATACCCTATATTG
	MY09/11	GCMCAGGGWCATAAYAATGG	CGTCCMARRGGAWACTGATC
	GP5+/6+	TTTGTTACTGTGGTAGATACTAC	GAAAAATAAACTGTAAATCATATTC
Multiple primers	PGMY09/11	GCACAGGGACATAACAATGG	CGTCCCAAAGGAAACTGATC
		GCGCAGGGCCACAATAATGG	CGACCTAAAGGAAACTGATC
		GCACAGGGACATAATAATGG	CGTCCAAAAGGAAACTGATC
		GCCCAGGGCCACAACAATGG	GCCAAGGGGAAACTGATC
		GCTCAGGGTTTAAACAATGG	CGTCCCAAAGGATACTGATC
			CGTCCAAGGGGATACTGATC
			CGACCTAAAGGGAATTGATC
			CGACCTAGTGGAAATTGATC
			CGACCAAGGGGATATTGATC
			GCCCAACGGAAACTGATC
			CGACCCAAGGGAAACTGGTC
			CGTCCTAAAGGAAACTGGTC
			GCGACCCAATGCAAATTGGT
	MGP	ACGTTGGATGTTTGTTACTGTGGTGGATACTAC	ACGTTGGATGGAAAAATAAACTGTAAATCATATTCCT
		ACGTTGGATGTTTGTTACCGTTGTTGATACTAC	ACGTTGGATGGAAAAATAAATTGTAAATCATACTC
		ACGTTGGATGTTTGTTACTAAGGTAGATACCACTC	ACGTTGGATGGAAATATAAATTGTAAATCAAATTC
		ACGTTGGATGTTTGTTACTGTTGTGGATACAAC	ACGTTGGATGGAAAAATAAACTGTAAATCATATTC
		ACGTTGGATGTTTGTTACTATGGTAGATACCACAC	ACGTTGGATGGAAAAATAAACTGCAAATCATATTC

MGP, modified GP5+/6+.

Fig. 1. Amplicons produced from the human papillomavirus (HPV)16*L1* gene by PCR with primers tested in this study. Both ends of amplicons are indicated by the nucleotide (nt) numbers of the HPV16*L1* gene. MGP, modified GP5+/6+.

describing the method.[5,17,18,20,21] Figure 1 shows the location of primers on the HPV16L1 ORF and the size of amplicons.

Reverse blotting hybridization. Reverse blotting hybridization was done as described previously.[22] Briefly, 15 μL denatured amplicons, of which the 5′-ends were labeled with biotin, were allowed to hybridize with the type-specific probes immobilized on a nylon membrane using the Miniblotter MN45 (Immunetics, Cambridge, MA, USA). The hybridized amplicon was detected using streptavidin–HRP (GE Healthcare Bio-Sciences, Piscataway, NJ, USA) and ECL detection reagents (GE Healthcare Bio-Sciences). The chemiluminescence was detected with the Light-Capture AE-6972 (ATTO, Tokyo, Japan). The intensities of dots were quantified by ImageJ software (National Institutes of Health, Bethesda, MD, USA). The specific density was calculated by the subtraction of the background from the integrated density. Samples showing the specific densities of more than 1000 intensity units were defined as positives.

The nucleotide sequences of type-specific probes for MY09/11, GP5+/6+, PGMY09/11, and MGP primers were described previously.[25,26] Type-specific probes for L1C1/L1C2+C2M primers were newly designed in this study. The nucleotide sequences were as follows: HPV16, 5′-GTTATTGTTAGGTTTTTTAA; HPV18, 5′-CCACCACCTGCAGGAACCCT; HPV31, 5′-AGGATTGTCAGATTTAGGTA; HPV51, 5′-TAGCAGCACGCGTTGAGGTT; HPV52, 5′-ACCATTACCACTACTGGTGT; and HPV58, 5′-TATTGTTATTGGGACTTTTG.

Real-time PCR. Copy numbers of HPV DNA in a clinical sample were determined by real-time PCR using type-specific primers and SYBR-green dye. A reaction mixture (20 μL) containing 2 μL sample, 10 μL Thunderbird SYBR qPCR Mix (Toyobo, Osaka, Japan), 0.4 μL ROX reference dye, and 0.9 μM each primer was subjected to PCR with the Applied Biosystems 7900HT (Life Technologies). The reaction was done in triplicate. The copy number was calculated with the standard curve obtained by using serially diluted HPV plasmids. The nucleotide sequences of type-specific primers are as follows: HPV16 forward, 5′-CAGAACCATATGGCGACAGC and reverse, 5′-GTACATTTTCACCAACAGCA; HPV18 forward, 5′-GATTATTTACAAATGTCTGCA and reverse, 5′-GCACAGTGTCACCCATAGTA; HPV31 forward, 5′-GATTATCTTAAAATGGTTGCT and reverse, 5′-GGACCGATTCACCAACCGTG; HPV51 forward, 5′-AGCTATGGATTTCGCTGCCC and reverse, 5′-AGCAAAGATTTGCTCCCTGC; HPV52 forward, 5′-GATTATTTGCAAATGGCTAGC and reverse, 5′-GGCACAGGGTCACCTAAGGTA; HPV58 forward, 5′-AGTGAACCTTATGGGGATAG and reverse, 5′-AAAGGTCATCCGGGA-

doi: 10.1111/j.1349-7006.2011.01922.x

CAGCC. Polymerase chain reaction with these primer sets amplified target HPV DNA without non-specific reaction. For example, PCR with the primers for HPV16 and a test sample containing HPV16 produced a single DNA fragment that formed a single peak in the dissociation curve.

Results

Amplification of HPV DNA in a test sample containing a single HPV genotype. Figure 2 shows the results of reverse blotting hybridization of the amplicons obtained by PCR from test samples (50 μL) containing 6, 60, 600, or 6000 copies of the plasmid having genomic DNA of HPV16, 18, 51, 52, and 58, all prevalent types among Japanese women, and 50 ng sheared human DNA. Three consensus primer pairs (L1C1/L1C2+C2M, MY09/11, and GP5+/6+) and two sets of mixed multiple primers (PGMY09/11 and MGP) were used for PCR. The biotinylated amplicons were allowed to hybridize with the type-specific probes immobilized on a nylon membrane and the biotin on the membrane was detected by streptavidin labeled with peroxidase.

Polymerase chain reaction with L1C1/L1C2+C2M produced detectable amplicons of HPV16, 18, 51, 52, and 58 from the samples containing 60, 6, 6, 60, and 60 copies of HPV DNA, respectively. Polymerase chain reaction with MY09/11 produced detectable amplicons of HPV16, 18, and 58 from the samples containing 600 copies of HPV DNA but did not produce detectable amplicons from the samples containing 6000 copies of HPV51 and 52. Polymerase chain reaction with GP5+/6+ produced detectable amplicons of HPV16, 18, 52, and 58 from the samples containing 60, 60, 6000, and 6000 copies, respectively, but failed to produce detectable amplicons from the sample containing 6000 copies of HPV51. Thus, PCR with L1C1/L1C2+C2M amplified HPV in the test samples more efficiently than the other PCR with the consensus primers.

Polymerase chain reaction with PGMY09/11 produced detectable amplicons of HPV16, 18, 51, 52, and 58 from the samples containing 6, 6, 60, 60, and 60 copies of HPV DNA, respectively. The PCR with MGP produced detectable amplicons of HPV16, 18, 51, 52, and 58 from samples containing 6, 60, 60, 6, and 600 copies of HPV DNA, respectively.

Amplification of HPV DNA in a mixed test sample containing HPV16, and either HPV18, 51, 52, or 58. Figure 3 shows the results of reverse blotting hybridization of the amplicons obtained by PCR from test samples containing 6000 copies of HPV16 and 6, 60, 600, and 6000 copies of either HPV18, 51, 52, or 58 and 50 ng sheared human DNA.

Polymerase chain reaction with L1C1/L1C2+C2M failed to amplify HPV16 DNA from the samples containing 6000 copies of HPV18 or 51 and the level of HPV16 amplicons was greatly reduced in the presence of 600 copies of HPV18 or 51. However, the amplification of HPV18 and 51 DNA was not influenced by the presence of 6000 copies of HPV16 DNA (Figs 2,3). The PCR with L1C1/L1C2+C2M amplified HPV16 DNA in the presence of HPV52 or 58 DNA. The data clearly indicate that amplification of HPV16 DNA by PCR with L1C1/L1C2+C2M was significantly interfered with by the presence of HPV18 or 51 DNA.

Polymerase chain reaction with MY09/11, GP5+/6+, PGMY09/11, or MGP amplified HPV16 DNA in the presence of HPV18, 51, 52, or 58 DNA but the level of HPV16 amplicons was reduced by co-existence of 6000 copies of HPV18 DNA. The PCR with GP5+/6+, PGMY09/11, or MGP produced reduced levels of HPV18, 52, or 58 amplicons in the co-existence of 6000 copies of HPV16 DNA (Figs 2,3).

Amplification of HPV DNA in clinical specimens containing two or three HPV genotypes. Table 2 shows the detection and genotyping of HPVs in clinical specimens using PCR with consensus primers. Eight clinical samples in which two or three HPV types had been detected by PCR with PGMY09/11 or MGP were selected, and the copy numbers of the detected HPV DNA in the samples were measured by real-time PCR using type-specific primers. Then the HPV in the samples was examined by PCR with L1C1/L1C2+C2M, MY09/11, or GP5+/6+. The HPV types detected with consensus primers are listed in decreasing order of amplicon levels.

In no. 165 containing HPV16 (16 000 copies), 18 (5200), and 31 (3100), HPV18 was detected by PCR with L1C1/L1C2+C2M but neither HPV16, which was three times more abundant than HPV18, nor 31 were detected. All three HPVs were detected by PCR with MY09/11. HPV16 and 18 were

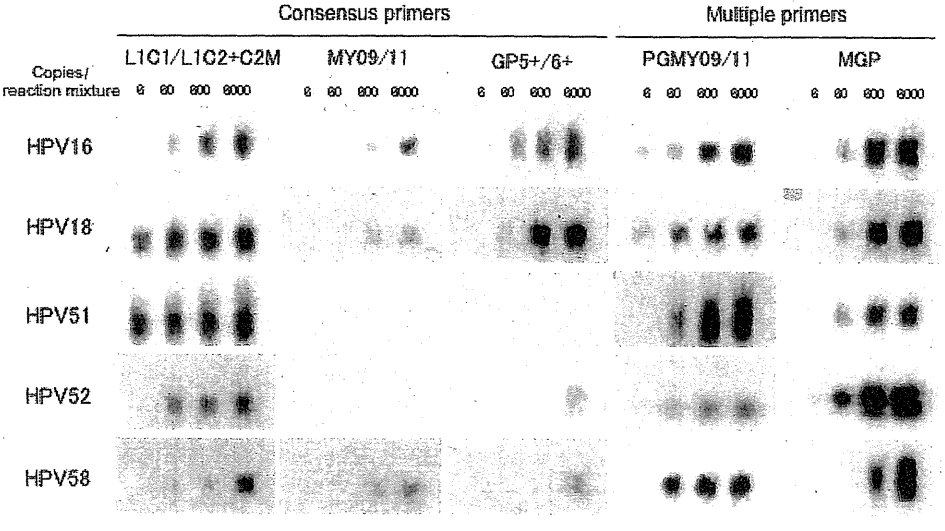

Fig. 2. Amplification of human papillomavirus (HPV) DNA in test samples containing HPV DNA of single genotype. The HPV DNA in the test sample was amplified by PCR with primers indicated. The test sample contained 6, 60, 600, or 6000 copies of plasmid DNA having HPV genomic DNA of the indicated type. The biotin-labeled amplified DNA fragments were hybridized with type-specific probes fixed on a membrane and reacted with streptavidin–HRP. MGP, modified GP5+/6+.

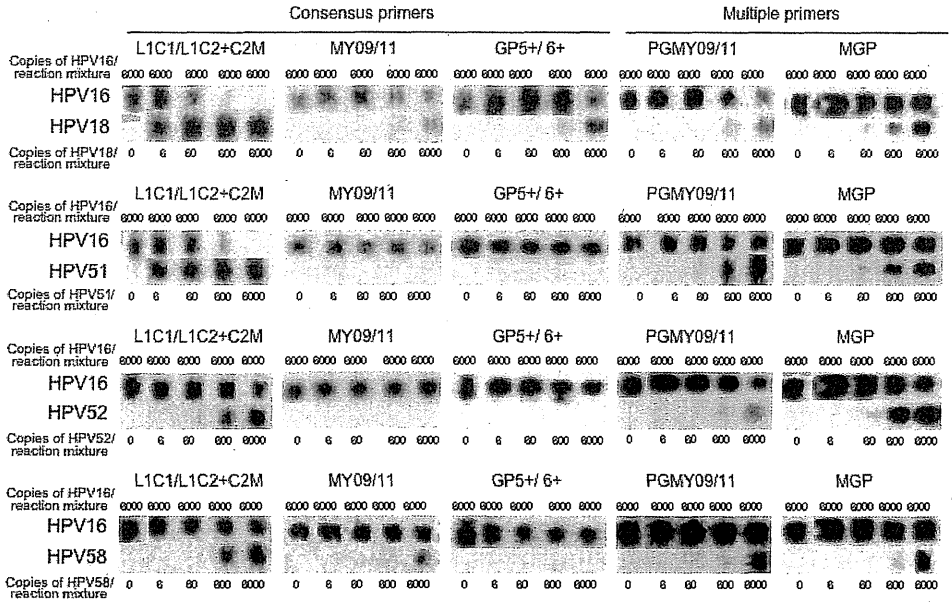

Fig. 3. Amplification of human papillomavirus (HPV) DNA in test samples containing HPV16 DNA and either HPV18, 51, 52, or 58 DNA. HPV DNA in the test sample was amplified by PCR with primers indicated. The test sample contained 6000 copies of HPV16 plasmid together with 6, 60, 600, or 6000 copies of HPV18, 51, 52, or 58 plasmid. The biotin-labeled amplified DNA fragments were hybridized with type-specific probes fixed on a membrane and reacted with streptavidin-horseradish peroxidase. MGP, modified GP5+/6+.

Table 2. Genotyping of clinical samples containing multiple types of human papillomavirus (HPV)

Sample no. (cytology)	Genotypes: copy numbers†	Consensus primers		
		L1C1/ L1C2+C2M	MY09/11	GP5+/6+
165 (CIN2)	16:16 000	18	18‡	16
	18:5200		16	18
	31:3100		31	
258 (CIN3)	52:1700	52	16	16
	16:1300	16	58	
	58:180	58		
352 (normal)	16:200		16	16
	52:25			
402 (CIN2)	52:7300	51	52	16
	51:120	52	16	
	16:110			
993 (CIN1)	16:5600	16	16	16
	52:3300	52		
996 (CIN1)	16:47 000	16	16	16
	52:25 000	52		
1061 (unknown)	18:4300	18	18	18
	16:290		16	16
1245 (CIN3)	16:78 000	58	58	16
	58:78 000	16	16	

†Genotypes detected using PGMY09/11 and modified GP5+/6+ primers. Copy numbers were determined by real-time PCR and expressed as copy numbers subjected to PCR for genotyping. ‡The HPV types detected with consensus primers are listed in decreasing order of amplicon levels.

detected by PCR with GP5+/6+ but HPV31, the least component, was not detected by PCR with GP5+/6+.

In no. 258 containing HPV52 (1700), 16 (1300), and 58 (180), all three HPVs were detected by PCR with L1C1/L1C2+C2M. HPV16 and 58 were detected by PCR with MY09/11 but HPV52, the most abundant type, was not detected. Only HPV16 was detected by PCR with GP5+/6+.

In no. 352 containing HPV16 (200) and 52 (25), neither HPVs were detected by PCR with L1C1/L1C2+C2M. Only HPV16 was detected by PCR with MY09/11 and PCR with GP5+/6+.

In no. 402 containing HPV52 (7300), 51 (120), and 16 (110), HPV16 was not detected by PCR with L1C1/L1C2+C2M. HPV16 and 52, but not HPV51, were detected by PCR with MY09/11. Only HPV16 was detected by PCR with GP5+/6+.

In no. 933 containing HPV16 (5600) and 52 (3300), and in no. 996 containing HPV16 (47 000) and 52 (25 000), HPV52 was not detected by PCR with MY09/11 and GP5+/6+.

In no. 1061 containing HPV18 (4300) and 16 (290), HPV16 was not detected by PCR with L1C1/L2C2+C2M.

In no. 1245 containing HPV16 (78 000) and 58 (78 000), HPV58 was not detected by PCR with GP5+/6+. Thus, amplification of HPV DNA in the clinical specimens containing multiple HPV genotypes by PCR with consensus primers was biased and sometimes caused misjudgment in typing.

Discussion

We evaluated HPV consensus primers for PCR amplification of HPV DNA in specimens containing multiple HPV types and concluded that PCR with consensus primers is not suitable for simultaneous amplification of multiple types of HPV DNA. The low sensitivity of HPV51 and 52 detection by PCR with MY09/11 and GP5+/6+ is consistent with previous reports.[20,21,27] Polymerase chain reaction with L1C1/L1C2+C2M, which amplified HPV DNA tested more efficiently than PCR with MY09/11 or GP5+/6+ (Fig. 2), failed to amplify HPV16 DNA when HPV18 or 51 DNA coexisted in the samples (Fig. 3, Table 2).

Polymerase chain reaction with L1C1/L1C2+C2M amplifies HPV18 and 51 DNA very efficiently, as shown in Figure 2. The resultant abundant HPV18 and 51 amplicons might inhibit reactions amplifying the other HPV types in the samples. Similarly, it is reported that interference in PCR was observed even

doi: 10.1111/j.1349-7006.2011.01922.x

between two closely related plant virus isolates that have identical binding sites for consensus primers, although the mechanism of the interference is not fully explained.[28]

As PCR with L1C1/L1C2+C2M has been used widely,[5–16] the biased amplification may have caused mistyping in the previous numerous studies of genotyping of clinical specimens. Previous studies using L1C1/L1C2+C2M showed that the rate of multiple infections among HPV-positive Japanese women was 10–20%.[15,16] In other countries, studies using PGMY09/11 showed that 30–45% of HPV-positive women were infected with multiple genotypes.[20,29–31] It is possible that reevaluation of HPV prevalence in Japanese women by using mixtures of type-specific primers, such as PGMY09/11 and MGP, increases the rate of multiple infections. The data of this study suggest that the genotyping data obtained by PCR with consensus primers should be carefully interpreted.

Acknowledgments

We acknowledge the World Health Organization's HPV Laboratory Network for technical transfer of reverse blotting hybridization into our laboratory. This work was supported by a grant-in-aid from the Ministry of Health, Labour and Welfare for the Third-Term Comprehensive 10-year Strategy for Cancer Control.

Disclosure Statement

The authors have no conflict of interest to declare.

References

1 Howley PM, Lowy DR. Papillomaviruses and their replication. In: Lnipe DM, Howley PM, eds. *Fields Virology*, Vol. 2, 4th edn. Philadelphia, PA: Lippincott, Williams and Wilkins, 2001; 2197–229.
2 Munoz N, Bosch FX, Castellsague X *et al.* Against which human papillomavirus types shall we vaccinate and screen? *Int J Cancer* 2004; **111**: 278–85.
3 Lacey CJ, Lowndes CM, Shah KV. Chapter 4: Burden and management of non-cancerous HPV-related conditions: HPV-6/11 disease. *Vaccine* 2006; **24**: S3/35–41.
4 Molijn A, Kleter B, Quint W, van Doorn LJ. Molecular diagnosis of human papillomavirus (HPV) infections. *J Clin Virol* 2005; **32**: S43–51.
5 Yoshikawa H, Kawana T, Kitagawa K, Mizuno M, Yoshikura H, Iwamoto A. Detection and typing of multiple genital human papillomaviruses by DNA amplification with consensus primers. *Jpn J Cancer Res* 1991; **82**: 524–31.
6 Iwasaka T, Matsuo N, Yokoyama M, Uchiyama K, Fukuda H, Sugimori H. Prospective follow-up of Japanese women with cervical intraepithelial neoplasia and various human papillomavirus types. *Int J Gynecol Obstet* 1998; **62**: 269–77.
7 Yoshikawa H, Nagata C, Noda K *et al.* Human papillomavirus infection and other risk factors for cervical intraepithelial neoplasia in Japan. *Br J Cancer* 1999; **80**: 621–4.
8 Maehama T, Asato T, Kanazawa K. Prevalence of HPV infection in cervical cytology-normal women in Okinawa, Japan, as determined by a polymerase chain reaction. *Int J Gynaecol Obstet* 2000; **69**: 175–6.
9 Maehama T, Asato T, Kanazawa K. Prevalence of human papillomavirus in cervical swabs in the Okinawa Islands, Japan. *Arch Gynecol Obstet* 2002; **267**: 64–6.
10 Masumoto N, Fujii T, Ishikawa M *et al.* Papanicolaou tests and molecular analyses using new fluid-based specimen collection technology in 3000 Japanese women. *Br J Cancer* 2003; **88**: 1883–8.
11 Asato T, Maehama T, Nagai Y, Kanazawa K, Uezato H, Kariya K. A large case-control study of cervical cancer risk associated with human papillomavirus infection in Japan, by nucleotide sequencing-based genotyping. *J Infect Dis* 2004; **189**: 1829–32.
12 Masumoto N, Fujii T, Ishikawa M *et al.* Dominant human papillomavirus 16 infection in cervical neoplasia in young Japanese women; study of 881 outpatients. *Gynecol Oncol* 2004; **94**: 509–14.
13 Maehama T. Epidemiological study in Okinawa, Japan, of human papillomavirus infection of the uterine cervix. *Infect Dis Obstet Gynecol* 2005; **13**: 77–80.
14 Takakuwa K, Mitsui T, Iwashita M *et al.* Studies on the prevalence of human papillomavirus in pregnant women in Japan. *J Perinat Med* 2006; **34**: 77–9.
15 Onuki M, Matsumoto K, Satoh T *et al.* Human papillomavirus infections among Japanese women: age-related prevalence and type-specific risk for cervical cancer. *Cancer Sci* 2009; **100**: 1312–6.
16 Matsumoto K, Oki A, Furuta R *et al.* Predicting the progression of cervical precursor lesions by human papillomavirus genotyping: a prospective cohort study. *Int J Cancer* 2010; doi: 10.1002/ijc.25630.
17 Manos MM, Ting Y, Wright DK, Lewis AJ, Broker TR, Wolinsky SM. The use of polymerase chain reaction amplification for the detection of genital human papillomaviruses. *Cancer Cell* 1989; **7**: 209–14.
18 de Roda Husman AM, Walboomers JM, van den Brule AJ, Meijer CJ, Snijders PJ. The use of general primers GP5 and GP6 elongated at their 3′ ends with adjacent highly conserved sequences improves human papillomavirus detection by PCR. *J Gen Virol* 1995; **76**: 1057–62.
19 Clifford GM, Smith JS, Plummer M, Muñoz N, Franceschi S. Human papillomavirus types in invasive cervical cancer worldwide: a meta-analysis. *Br J Cancer* 2003; **88**: 63–73.
20 Gravitt PE, Peyton CL, Alessi TQ *et al.* Improved amplification of genital human papillomaviruses. *J Clin Microbiol* 2000; **38**: 357–61.
21 Söderlund-Strand A, Carlson J, Dillner J. Modified general primer PCR system for sensitive detection of multiple types of oncogenic human papillomavirus. *J Clin Microbiol* 2009; **47**: 541–6.
22 World Health Organization, Department of Immunization, Vaccines and Biologicals. Human papillomavirus laboratory manual, 1st edn. 2009. Available from URL: http://www.who.int/biologicals/vaccines/hpv/en/index.html.
23 Mendez F, Munoz N, Posso H *et al.* Cervical coinfection with human papillomavirus (HPV) types and possible implications for the prevention of cervical cancer by HPV vaccines. *J Infect Dis* 2005; **192**: 1158–65.
24 Schmitt M, Dondog B, Waterboer T, Pawlita M, Tommasino M, Gheit T. Abundance of multiple high-risk human papillomavirus (HPV) infections found in cervical cells analyzed by use of an ultrasensitive HPV genotyping assay. *J Clin Microbiol* 2010; **48**: 143–9.
25 Gravitt PE, Peyton CL, Apple RJ, Wheeler CM. Genotyping of 27 human papillomavirus types by using L1 consensus PCR products by a single-hybridization, reverse line blot detection method. *J Clin Microbiol* 1998; **36**: 3020–7.
26 Schmitt M, Bravo IG, Snijders PJ, Gissmann L, Pawlita M, Waterboer T. Bead-based multiplex genotyping of human papillomaviruses. *J Clin Microbiol* 2006; **44**: 504–12.
27 Chan PK, Cheung TH, Tam AO *et al.* Biases in human papillomavirus genotype prevalence assessment associated with commonly used consensus primers. *Int J Cancer* 2006; **118**: 243–5.
28 Rosner A, Maslenin L. Interference in PCR: transcription amplifications of mixed PVY isolates. *Plant Prot Sci* 2005; **41**: 125–31.
29 Coutlée F, Gravitt P, Kornegay J *et al.* Use of PGMY primers in L1 consensus PCR improves detection of human papillomavirus DNA in genital samples. *J Clin Microbiol* 2002; **40**: 902–7.
30 Klug SJ, Hukelmann M, Hollwitz B *et al.* Prevalence of human papillomavirus types in women screened by cytology in Germany. *J Med Virol* 2007; **79**: 616–25.
31 van Doorn LJ, Quint W, Kleter B *et al.* Genotyping of human papillomavirus in liquid cytology cervical specimens by the PGMY line blot assay and the SPF(10) line probe assay. *J Clin Microbiol* 2002; **40**: 979–83.

International Journal of Gynecological Pathology
30:30–35, Lippincott Williams & Wilkins, Baltimore

Original Article

Rsf-1 (HBXAP) Expression is Associated With Advanced Stage and Lymph Node Metastasis in Ovarian Clear Cell Carcinoma

Daichi Maeda, M.D., Xu Chen, M.D., Bin Guan, Ph.D., Shunsuke Nakagawa, M.D., Ph.D., Tetsu Yano, M.D., Ph.D., Yuji Taketani, M.D., Ph.D., Masashi Fukayama, M.D., Ph.D., Tian-Li Wang, Ph.D., and Ie-Ming Shih, M.D., Ph.D.

Summary: Ovarian clear cell carcinoma (CCC) is a unique type of ovarian cancer characterized by distinct clinicopathological and molecular features. CCC is considered to be a highly malignant disease because it is resistant to conventional chemotherapy, and when presented at advanced stages, it has a dismal overall survival. Identifying and characterizing biomarkers associated with its malignant behavior is fundamental toward elucidating the mechanisms underlying its aggressive phenotype. In this study, we performed immunohistochemical analysis on 89 CCCs to assess their expression of Rsf-1 (HBXAP), a chromatin-remodeling gene frequently amplified and overexpressed in several types of human cancer. We found that 73 (82%) of the 89 CCCs expressed Rsf-1 and most importantly, there was a statistically significant correlation between Rsf-1 immunostaining intensity and the 2 disease parameters: advanced stage ($P=0.008$) and status of retroperitoneal lymph node metastasis ($P=0.023$). However, there was no correlation between Rsf-1 expression and patient age, peritoneal tumor dissemination, or overall survival. In conclusion, a higher expression level of Rsf-1 is associated with advanced clinical stage and lymph node metastasis in CCC. Our data suggest that Rsf-1 participates in tumor progression in CCC, and indicates that the contribution of Rsf-1 to disease aggressiveness deserves further study. **Key Words:** Rsf-1–HBXAP–Ovarian cancer—Clear cell carcinoma.

Ovarian clear cell carcinoma (CCC) represents less than 10% of ovarian cancers in the United States, but occurs more frequently in Asian women (1,2). Multivariate analysis on a large series of CCC shows that women with CCC present at a younger age and at earlier clinical stages as compared with high-grade (conventional) serous carcinoma, the most common and lethal type of ovarian cancer (1). Approximately 50% of CCCs present as stage I diseases (3,4), and despite being diagnosed at an early stage, are generally considered to be highly malignant (5). Morphologic and molecular studies have shown that many CCCs develop in a stepwise manner from endometriosis through atypical endometriosis to overt CCC (6–10). In fact, CCC is the most common ovarian carcinoma associated with endometriosis. There has been increased enthusiasm for identifying markers that are predictive of the clinical outcome in CCC patients. This is because CCC typically presents with stage I or II disease, and prognostic markers could have an impact on clinical decision making in the management of CCC patients, such as administration of adjuvant

From the Department of Pathology (D.M., X.C., B.G., I-M.S.); Departments of Gynecology and Obstetrics and Oncology (D.M., T-L.W., I-M.S.), Johns Hopkins Medical Institutions, Baltimore, Maryland; Department of Pathology (D.M., M.F.); and Department of Obstetrics and Gynecology (S.N., T.Y., Y.T.), Graduate School of Medicine, the University of Tokyo, Tokyo, Japan.

This study was supported by NIH/NCI Grant CA129080 and the International Training Program from the Japan Society for the Promotion of Science.

Address correspondence and reprint requests to Ie-Ming Shih, MD, PhD, Johns Hopkins Medical Institutions, 1550 Orleans street, CRB-2, room: 305, Baltimore, Maryland 21231. E-mail: ishih@jhmi.edu.

DOI: 10.1097/PGP.0b013e3181e9a319

chemotherapy. For example, IGF2BP3 (IMP3) expression has been reported to be an independent marker of reduced disease-specific survival in CCC, but not in high-grade serous or endometrioid carcinomas of the ovary (11). Similarly, enhanced expression of annexin A4 in CCC and its association with chemoresistance to carboplatin have been recently reported (12).

To further identify markers that are associated with poor prognosis in CCC and to explore the molecular mechanisms that account for the aggressive behavior of CCC, we determined the correlation between immunoreactivity of Rsf-1, also known as HBXAP, and clinical outcome in primary CCCs. We focused on Rsf-1 (HBXAP) because the encoded protein participates in chromatin remodeling, and this gene has been identified as an amplified gene with a tumor-promoting potential in several types of neoplastic diseases including ovarian high-grade serous carcinoma (13–15). Our analysis showed that the higher expression levels of Rsf-1 (HBXAP) were associated advanced stage disease and retroperitoneal lymph node metastasis. This study provides new evidence of the biological significance of Rsf-1 expression in CCC.

MATERIALS AND METHODS

Tissue Samples

Formalin-fixed and paraffin-embedded CCC tissues were obtained from the Department of Pathology at the University of Tokyo Hospital. A total of 89 cases of primary CCCs were retrieved from the archives, and hematoxylin and eosin-stained slides were reviewed to confirm the diagnosis based on the most recent criteria of the World Health Organization. The CCC tissues were arranged in tissue microarrays (Beecher Instruments, Silver Spring, MD) with duplicate 2 mm tissue cores obtained from the tumor area in each CCC. The collection of clinical specimens was in compliance with the guidelines of tissue procurement at the University of Tokyo Hospital.

Clinical Information of Patients With Ovarian CCC

We reviewed the medical records of all the 89 CCC patients; data obtained included demographics, age at the time of diagnosis, preoperative diagnosis, clinical stage, and survival time after treatment. None of the patients underwent preoperative chemotherapy or radiotherapy. The correlations of Rsf-1 expression with the following clinical variables were evaluated: age, stage of carcinoma (stage I/II vs. stage III/IV), peritoneal dissemination, retroperitoneal lymph node metastasis, and death rate. The stage of carcinoma was assessable in 67 cases in which the appropriate staging procedures were performed; the remaining 22 cases were not included in the staging analysis because of either incomplete surgical procedures or missing data. Staging was in accordance with the standards of the International Federation of Gynecology and Obstetrics. Comprehensive evaluation of peritoneal dissemination that included microscopic examination of the omentum, peritoneal wall and mesentery soft tissues was performed in 79 cases. Retroperitoneal lymph node dissection was performed in 70 cases. Follow-up information included overall survival and cancer-related death. The follow-up interval was calculated from the date of surgery to the date of death or last clinical evaluation. The mean follow-up interval was 50 months (range, 1–196 mo).

Immunohistochemistry

The method of immunohistochemistry and scoring of immunoreactivity for Rsf-1 expression were described earlier (13,14). In brief, 4 μm sections were cut from the tissue microarray blocks. Antigen retrieval was performed on the deparaffinized sections by steaming them in citrate buffer (pH 6.0). A monoclonal anti-Rsf-1 antibody, clone 5H2/E4 (Upstate, Lake Placid, NY) was used at an optimal dilution of 1:2000 as determined earlier (13,14) and a monoclonal anti-NAC1 antibody was used at a dilution of 1:250 (16). The sections were incubated with the antibodies for 2 hours at room temperature, followed by the EnVision+ System (Dako, Carpinteria, CA) using the peroxidase method. An isotype-matched control antibody (MN-4) was used in parallel (17). Our earlier studies had shown that the distribution of Rsf-1 immunoreactivity was always homogeneous within a tumor; therefore, we used an intensity score ranging from 0 to 4+ to evaluate Rsf-1 immunoreactivity in tumors as described earlier (14). A positive reaction for both Rsf-1 and NAC1 was defined as discrete localization of the chromogen in the nuclei. The tissues were scored in a blinded manner without the knowledge of clinical information.

Rsf-1 Gene Knockdown Using Small Hairpin RNA

Ovarian clear cell adenocarcinoma cell lines, ES2 and JHOC5, were used in this study. ES2 was

obtained from the American Type Culture Collection (Rockville, MD); JHOC5 was a gift from Dr Kentaro Nakayama, Shimane University, Japan. Both the cell lines used in this study were cultured in RPMI 1640 containing 5% fetal bovine serum.

To confirm the specificity of the anti-Rsf-1 antibody used for immunohistochemistry, we performed Rsf-1 knockdown by transduction of 2 small hairpin RNAs (shRNA) and evaluated the knockdown efficiency by Western blot analysis. The antibody specificity was indicated by reduced protein expression corresponding to Rsf-1 after the gene knockdown based on the western blot analysis using the same anti-Rsf-1 antibody as used in immunohistochemistry. We used a lentivirus carrying the Rsf-1 shRNA sequence templates (CCGGCCAGTTCTGAACTTTGAAGATCTCGAGATCTTCAAAGTTCAGAACT) and (CCGGCTTCTGAGACAAAGGGTTCTACTCGAGTAGAACCCTTTGTCTCAGA), and a control shRNA sequence template, which were inserted into the lentiviral plasmid (pLKO.1-puro). The cells were washed and harvested 24 hours after transfection for protein and mRNA extraction.

For Western blot analysis, the protein lysates were separated by 4% to 20% Tris-glycine gel electrophoresis and transferred onto polyvinylidene difluoride membranes using a semidry apparatus (Bio-Rad). After blocking, the membranes were incubated with the anti-Rsf-1 (clone 5H2/E4) primary antibody at 4°C overnight followed by incubation with horseradish peroxidase-conjugated secondary antibody. Protein bands were detected with Amersham ECL Western blotting detection reagents (GE Healthcare). Antibody reacting to anti-glyceraldehyde-3-phosphate dehydrogenase was used to evaluate the amount of glyceraldehyde-3-phosphate dehydrogenase as a loading control. Western blot analysis showed a reduced protein band corresponding to Rsf-1 in the cells transfected with Rsf-1 shRNA as compared with the control shRNA-transfected cells, indicating the specificity of the anti-Rsf-1 antibody (Fig. 1).

Statistical Analysis

Statistical analysis was performed using the χ^2 test. Overall survival of the CCC cases was calculated using the Kaplan-Meier method, and statistical analyses were performed using the log-rank test. Statistical analyses were performed using the StatView 5.0 software (SAS Institute, Cary, NC) and a $P<0.05$ was considered statistically significant.

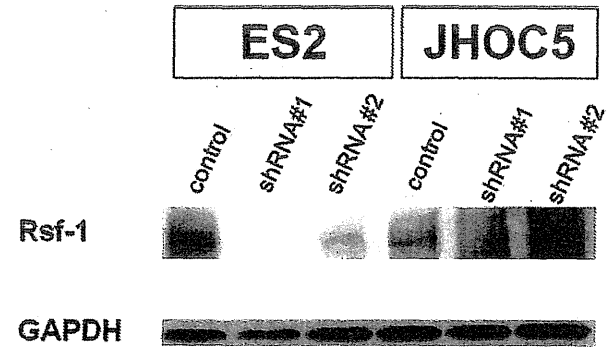

FIG. 1. Rsf-1 expression in ovarian clear cell carcinoma cell lines, ES2 and JHOC5. Western blot analysis showed a reduced protein band corresponding to Rsf-1 protein in the Rsf-1-specific shRNA-transfected cells as compared with the control shRNA-transfected cells, indicating the specificity of the anti-Rsf-1 antibody. GAPDH indicates glyceraldehyde-3-phosphate dehydrogenase.

RESULTS

Expression of Rsf-1 in Ovarian CCCs

Results of Rsf-1 immunohistochemistry in CCCs are summarized in Table 1. Rsf-1 immunoreactivity was detected exclusively in the nuclei of almost all the tumor cells. Positive immunoreactivity of Rsf-1 was observed in 73 (82%) of the 89 cases. Specifically, 16 (18%), 53 (60%), and 19 (21%) of the 89 cases had a staining score of 0, 1+, and 2+, respectively. Only 1 case exhibited intense nuclear staining (3+). Histologic features in the representative cases with different Rsf-1 immunostaining intensities including 0, 1+, and 2+ are shown in Figure 2. There was no correlation between Rsf-1 expression and the histological pattern and nuclear atypia of the CCC cases.

Correlation of Rsf-1 Expression With Clinical Features

As Rsf-1 expression has been reported to play a tumor-promoting role in ovarian cancer, we analyzed the possible correlation of Rsf-1 expression with clinical characteristics in CCC (Table 2). Statistically significant correlations were observed between Rsf-1 immunostaining intensity (score > 1) and lymph

TABLE 1. *Rsf-1 expression in ovarian clear cell carcinoma*

Immunostaining intensity score	No. cases	%
0	16	18
1+	53	60
2+	19	21
3+	1	1
4+	0	0
Total	89	100

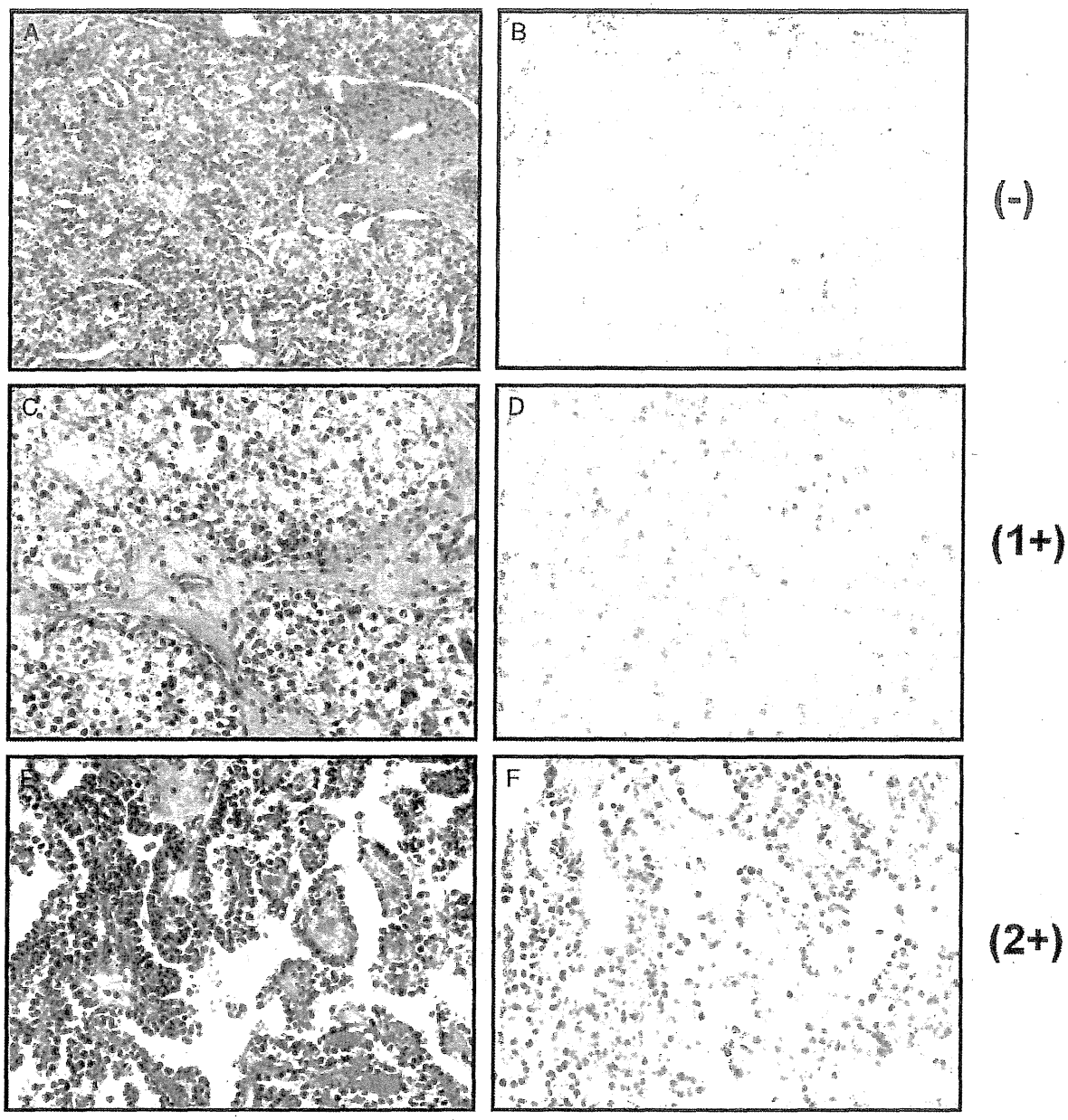

FIG. 2. Rsf-1 immunoreactivity in representative ovarian clear cell carcinomas. (A, B) Microscopic view of an ovarian clear cell carcinoma showing negative immunoreactivity for Rsf-1. (C, D) A case of ovarian clear cell carcinoma with 1+ immunostaining intensity for Rsf-1. (E, F) A clear cell carcinoma with 2+ immunoreactivity for Rsf-1. A, C, and E: hematoxylin and eosin-stained sections; B, D, and F: Rsf-1-stained sections.

node involvement ($P=0.023$). Furthermore, Rsf-1 immunostaining intensity (score >1) was associated with advanced stage disease (stage III/IV) ($P=0.0088$). In fact, none of the Rsf-1-negative cases presented at an advanced stage. The frequency of peritoneal dissemination was higher in the Rsf-1-positive cases (12 of 65) compared with the Rsf-1-negative cases (1 of 14), but the difference was not statistically significant ($P=0.3$). As a control we also assessed the expression of Nac1, a nuclear protein involved in transcription regulation, in the same set of CCCs. We found that there was no significant association between Nac1 expression and any clinical feature including presentation stage or lymph node metastasis status ($P>0.1$) (data not shown). Kaplan-Meier analyses were performed to determine if there was a correlation between Rsf-1 expression and clinical outcome. We first assessed the association

TABLE 2. *Correlation of Rsf-1 expression with clinical characteristics in ovarian clear cell carcinomas*

	Rsf-1 (HBXAP) expression		
Clinical characteristics	Positive	Negative	*P*
Age (n = 89)			
≥50	46 (79%)	12 (21%)	
<50	27 (87%)	4 (13%)	0.36
Stage (n = 67)			
I, II	34 (72%)	13 (28%)	
III, IV	20 (100%)	0 (0%)	0.0088*
Peritoneal dissemination (n = 79)			
Negative	53 (80%)	13 (20%)	
Positive	12 (92%)	1 (8%)	0.30
Lymph node metastasis (n = 70)			
Negative	40 (73%)	15 (27%)	
Positive	15 (100%)	0 (0%)	0.023*
Survival status (n = 89)			
Alive	58 (81%)	14 (19%)	
Deceased	15 (88%)	2 (12%)	0.46

*Statistically significant.

between tumor stage and overall survival in the CCCs, and observed that the stage III/IV cases (n = 20) had a poorer prognosis than the stage I/II cases (n = 47) ($P < 0.0001$) (Fig. 3). However, the Kaplan-Meier analysis did not show a significant difference in survival between the Rsf-1-positive and negative cases ($P = 0.42$).

DISCUSSION

An increase in the DNA copy number at the chromosome 11q13.5 locus containing Rsf-1 (HBXAP) is detected in several types of human cancers including ovarian high-grade serous carcinoma. Rsf-1 (HBXAP) encodes for a cellular nuclear protein that binds to hSNF2H (18), forming a chromatin-remodeling protein complex called RSF (remodeling and spacing factor) (19,20). Rsf-1 (HBXAP) has been shown to function as a histone chaperone in the nuclei, whereas its binding partner, hSNF2H, possesses nucleosome-dependent ATPase activity (21). The Rsf-1/hSNF2H complex (RSF complex) mediates ATP-dependent chromatin remodeling, which alters the chromatin structure or positioning of nucleosomes (20). At the cellular level, RSF participates in chromatin remodeling in response to a variety of growth signals and environmental cues. Such nucleosome remodeling is required for transcriptional activation or repression (22–24), DNA replication (25), and cell cycle progression (26).

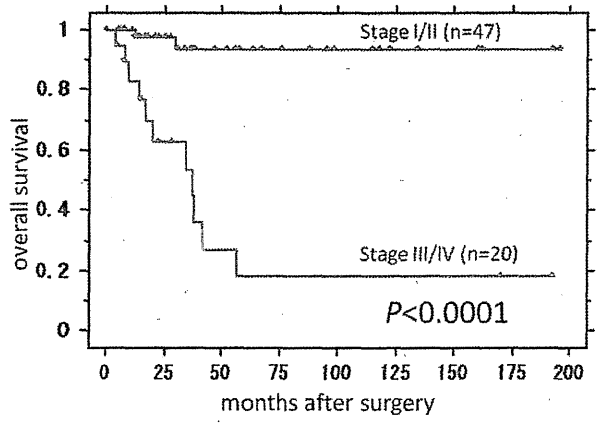

FIG. 3. Kaplan-Meier survival curve analysis shows that patients with stage III/IV ovarian clear cell carcinoma have a significantly worse overall survival rate than those with stage I/II ovarian clear cell carcinoma ($P < 0.0001$).

In this study, we used a well-characterized anti-Rsf-1 antibody to study the expression pattern of Rsf-1 in CCC, and provided new evidence that the expression of Rsf-1 was associated with advanced clinical stages and with the status of lymph node metastasis in CCC. The findings suggest a biological role for Rsf-1 in disease aggressiveness in this type of ovarian carcinoma. Interestingly, we have reported earlier that chromosome 11q13.5 amplification and overexpression in the cases of ovarian high-grade serous carcinoma contribute to a shorter overall survival compared with the cases without amplification. A possible mechanism was thought to be related to the *de novo* paclitaxel resistance rendered by Rsf-1 overexpression (27). Although the Kaplan-Meier survival analysis did not show a statistically significant difference between the Rsf-1-positive CCC cases and the Rsf-1-negative CCC cases, long-term prognosis of the Rsf-1-positive cases seems to be slightly worse than the Rsf-1-negative cases. However, the number of Rsf-1-negative CCC cases in our series was relatively small, and we believe that analysis in a larger series on CCCs is required to conclude if Rsf-1 overexpression predicts worse overall survival in CCCs. Furthermore, our study suggests a potential use of Rsf-1 immunoreactivity as a biomarker, which may prove useful for predicting clinical outcomes in primary CCC, including higher clinical stages, and for predicting the risk of developing lymph node metastasis. To this end, several proteins including IGF2BP3 (IMP3) (11) and annexin A4 (12) have been reported as new markers associated with the treatment outcomes in CCC. Thus, a panel of different markers including Rsf-1 could be tested in future clinical trials to determine their potential for use in the management of CCC patients.

In this report, we observed that with a single exception, the immunostaining intensity score of Rsf-1 was less than 3+ in all the cases analyzed.

This finding provides an independent confirmation of our earlier observation in another, smaller set of CCC samples in which we observed that the majority of CCCs showed an immunostaining intensity score of 1+ or 2+ (14). In fact, the percentage of Rsf-1-positive and negative cases is very similar between this and the earlier report. Moreover, analysis of single nucleotide polymorphism arrays performed on affinity-purified CCC specimens did not show an increase in the DNA copy number at chromosome 11q13.5, indicating that Rsf-1 is rarely amplified in CCC (28). The above findings in CCC are in sharp contrast to those in high-grade serous carcinoma (14), and underscore the distinct molecular pathways in developing CCC and high-grade serous carcinoma [reviewed in Ref. (29)]. It is also noteworthy that endometrioid and mucinous carcinomas of the ovary express Rsf-1 much less frequently as compared with CCCs and high-grade serous carcinoma. Only 49% of endometrioid carcinomas and 48% of mucinous carcinomas were Rsf-1 positive, and the intensity scores of the positive cases were mostly 1+ and 2+.

In conclusion, using immunohistochemistry with an Rsf-1-specific antibody we showed that the presence of Rsf-1 immunoreactivity is significantly associated with advanced stage and lymph node metastasis in primary CCCs. Our findings suggest that Rsf-1 expression may contribute to disease aggressiveness in CCC, and warrant further study of the biological role of Rsf-1 in the progression of CCC.

REFERENCES

1. Chan JK, Teoh D, Hu JM, et al. Do clear cell ovarian carcinomas have poorer prognosis compared to other epithelial cell types? A study of 1411 clear cell ovarian cancers. *Gynecol Oncol* 2008;109:370–6.
2. Ushijima K. Current status of gynecologic cancer in Japan. *J Gynecol Oncol* 2009;20:67–71.
3. Takano M, Kikuchi Y, Yaegashi N, et al. Clear cell carcinoma of the ovary: a retrospective multicentre experience of 254 patients with complete surgical staging. *Br J Cancer* 2006;94:1369–74.
4. Mizuno M, Kikkawa F, Shibata K, et al. Long-term follow-up and prognostic factor analysis in clear cell adenocarcinoma of the ovary. *J Surg Oncol* 2006;94:138–43.
5. Jenison EL, Montag AG, Griffiths CT, et al. Clear cell adenocarcinoma of the ovary: a clinical analysis and comparison with serous carcinoma. *Gynecol Oncol* 1989;32:65–71.
6. Veras E, Mao TL, Ayhan A, et al. Cystic and adenofibromatous clear cell carcinomas of the ovary: distinctive tumors that differ in their pathogenesis and behavior: a clinicopathologic analysis of 122 cases. *Am J Surg Pathol* 2009;33:844–53.
7. Fukunaga M, Nomura K, Ishikawa E, et al. Ovarian atypical endometriosis: its close association with malignant epithelial tumours. *Histopathology* 1997;30:249–55.
8. Erzen M, Rakar S, Klancnik B, et al. Endometriosis-associated ovarian carcinoma (EAOC): an entity distinct from other ovarian carcinomas as suggested by a nested case-control study. *Gynecol Oncol* 2001;83:100–8.
9. Sato N, Tsunoda H, Nishida M, et al. Loss of heterozygosity on 10q23.3 and mutation of the tumor suppressor gene PTEN in benign endometrial cyst of the ovary: possible sequence progression from benign endometrial cyst to endometrioid carcinoma and clear cell carcinoma of the ovary. *Cancer Res* 2000;60:7052–6.
10. Marquez RT, Baggerly KA, Patterson AP, et al. Patterns of gene expression in different histotypes of epithelial ovarian cancer correlate with those in normal fallopian tube, endometrium, and colon. *Clin Cancer Res* 2005;11:6116–26.
11. Kobel M, Xu H, Bourne PA, et al. IGF2BP3 (IMP3) expression is a marker of unfavorable prognosis in ovarian carcinoma of clear cell subtype. *Mod Pathol* 2009;22:469–75.
12. Aoki D, Oda Y, Hattori S, et al. Overexpression of class III beta-tubulin predicts good response to taxane-based chemotherapy in ovarian clear cell adenocarcinoma. *Clin Cancer Res* 2009;15:1473–80.
13. Shih IM, Sheu JJ, Santillan A, et al. Amplification of a chromatin remodeling gene, Rsf-1/HBXAP, in ovarian carcinoma. *Proc Natl Acad Sci U S A* 2005;102:14004–9.
14. Mao TL, Hsu CY, Yen MJ, et al. Expression of Rsf-1, a chromatin-remodeling gene, in ovarian and breast carcinoma. *Hum Pathol* 2006;37:1169–75.
15. Shih IM, Davidson B. Pathogenesis of ovarian cancer: clues from selected overexpressed genes. *Future Oncol* 2009;5:1641–57.
16. Nakayama K, Nakayama N, Davidson B, et al. A BTB/POZ protein, NAC-1, is related to tumor recurrence and is essential for tumor growth and survival. *Proc Natl Acad Sci U S A* 2006; 103:18739–44.
17. Shih IM, Nesbit M, Herlyn M, et al. A new Mel-CAM (CD146)-specific monoclonal antibody, MN-4, on paraffin-embedded tissue. *Mod Pathol* 1998;11:1098–106.
18. Sheu JJ, Choi JH, Yildiz I, et al. The roles of human sucrose nonfermenting protein 2 homologue in the tumor-promoting functions of Rsf-1. *Cancer Res* 2008;68:4050–7.
19. LeRoy G, Loyola A, Lane WS, et al. Purification and characterization of a human factor that assembles and remodels chromatin. *J Biol Chem* 2000;275:14787–90.
20. Loyola A, Huang J-Y, LeRoy G, et al. Functional analysis of the subunits of the chromatin assembly factor RSF. *Mol Cell Biol* 2003;23:6759–68.
21. Aihara T, Miyoshi Y, Koyama K, et al. Cloning and mapping of SMARCA5 encoding hSNF2H, a novel human homologue of Drosophila ISWI. *Cytogenet Cell Genet* 1998;81:191–3.
22. Shamay M, Barak O, Shaul Y. HBXAP, a novel PHD-finger protein, possesses transcription repression activity. *Genomics* 2002;79:523–9.
23. Shamay M, Barak O, Doitsh G, et al. Hepatitis B virus pX interacts with HBXAP, a PHD finger protein to coactivate transcription. *J Biol Chem* 2002;277:9982–8.
24. Vignali M, Hassan AH, Neely KE, et al. ATP-dependent chromatin-remodeling complexes. *Mol Cell Biol* 2000;20: 1899–910.
25. Flanagan JF, Peterson CL. A role for the yeast SWI/SNF complex in DNA replication. *Nucleic Acids Res* 1999;27:2022–8.
26. Cosma MP, Tanaka T, Nasmyth K. Ordered recruitment of transcription and chromatin remodeling factors to a cell cycle- and developmentally regulated promoter. *Cell* 1999;97:299–311.
27. Choi JH, Sheu JJ, Guan B, et al. Functional analysis of 11q13.5 amplicon identifies Rsf-1 (HBXAP) as a gene involved in paclitaxel resistance in ovarian cancer. *Cancer Res* 2009;69: 1407–15.
28. Kuo K, Mao T, Feng Y, et al. DNA copy number profiles in affinity-purified ovarian clear cell carcinoma. *Clin Cancer Res* 2010;16:1996–2008.
29. Cho KR, Shih IM. Ovarian cancer. *Annu Rev Pathol Mech Dis* 2009;4:287–313.

Virchows Arch (2010) 457:597–608
DOI 10.1007/s00428-010-0979-4

ORIGINAL ARTICLE

Mucosal carcinoma of the fallopian tube coexists with ovarian cancer of serous subtype only: a study of Japanese cases

Daichi Maeda · Satoshi Ota · Yutaka Takazawa · Kenichi Ohashi · Masaya Mori · Tetsuo Imamura · Shunsuke Nakagawa · Tetsu Yano · Yuji Taketani · Masashi Fukayama

Received: 1 June 2010 / Revised: 7 September 2010 / Accepted: 10 September 2010 / Published online: 25 September 2010

Abstract Previous studies in Western countries have revealed that mucosal carcinoma of the fallopian tube frequently coexists with pelvic (ovarian, tubal, and peritoneal) serous carcinomas, and early tubal carcinoma is now regarded as a possible origin of these tumors. However, the relationship between early tubal carcinoma and non-serous ovarian cancer, such as clear cell adenocarcinoma, has not been studied in detail. In this study, we sought to examine the coexistence of mucosal carcinoma of the fallopian tube in Japanese ovarian cancer cases. We submitted the fallopian tubes in toto for histological examination in 52 ovarian carcinoma cases and three peritoneal serous carcinoma cases. The ovarian tumors included 12 serous adenocarcinomas, 23 clear cell adenocarcinomas, nine endometrioid adenocarcinomas, three mucinous adenocarcinomas, and four mixed epithelial carcinomas. Mucosal carcinoma of the fallopian tube did not coexist with non-serous adenocarcinoma (n=40). In contrast, mucosal carcinoma of the fallopian tube was observed in six cases of ovarian serous adenocarcinoma and one case of peritoneal serous adenocarcinoma. In these cases, the p53 immunophenotypes were similar in tubal lesions and invasive ovarian or peritoneal carcinomas. Tumors were negative for p53 in four of seven cases, and one of the p53-negative serous adenocarcinomas showed low-grade morphology. We believe that some ovarian and peritoneal serous adenocarcinomas develop from early tubal carcinomas. However, it should be noted that early tubal carcinomas are not always p53-positive immunohistochemically. Finally, it is unlikely that early tubal lesions are involved in the carcinogenesis of clear cell adenocarcinoma and other non-serous adenocarcinomas.

Keywords Ovarian carcinoma · Fallopian tube · Mucosal carcinoma · p53

D. Maeda · S. Ota · Y. Takazawa · M. Fukayama (✉)
Department of Pathology, Graduate School of Medicine,
The University of Tokyo,
7-3-1 Hongo Bunkyoku,
Tokyo 113-0033, Japan
e-mail: mfukayama-tky@umin.net

K. Ohashi
Department of Pathology, Toranomon Hospital,
2-2-2 Toranomon Minato-ku,
Tokyo, Japan

M. Mori
Department of Pathology, Mitsui Memorial Hospital,
1 Kandaizumicho Chiyoda-ku,
Tokyo, Japan

T. Imamura
Department of Pathology, Teikyo University Hospital,
2-11-1 Kaga Itabashi-ku,
Tokyo, Japan

S. Nakagawa · T. Yano · Y. Taketani
Department of Obstetrics and Gynecology,
Graduate School of Medicine, The University of Tokyo,
7-3-1 Hongo Bunkyo-ku,
Tokyo, Japan

Introduction

The pathogenesis of primary ovarian carcinomas has long been controversial, and it remains a topic of debate. Ovarian surface epithelium or intracortical inclusion cysts have been considered to be the origin of most ovarian carcinomas, and thus, the term "malignant surface epithelial tumor" has been used to represent ovarian carcinoma [1]. It is also known that some endometrioid adenocarcinomas

and clear cell adenocarcinomas arise from endometriotic lesions [2–4]. At this point, regarding mucinous adenocarcinomas and low-grade serous adenocarcinomas, stepwise carcinogenesis from borderline tumor to invasive carcinoma has been suggested. In contrast, high-grade serous adenocarcinoma, which often presents in an advanced stage with multiple peritoneal disseminations, is believed to arise de novo, and *TP53* mutation is known to play a key role in its progression [5, 6].

In recent years, accumulating evidence suggests that the fallopian tube epithelium is the origin of the tumors conventionally diagnosed as ovarian high-grade serous adenocarcinomas [7–15]. This novel theory has attracted much attention in the field of gynecological research. Three major findings were essential to establishing this theory. First, extensive sectioning of salpingo-oophorectomy specimens from women with BRCA mutations has shown that the fallopian tube, especially its fimbriated end, is a preferred site for early adenocarcinoma [9, 16–18]. These early forms of tubal adenocarcinoma were usually in situ lesions, and Crum et al. referred to them as "tubal intraepithelial carcinomas" (TICs) [7, 10]. Second, histological examination of the whole fallopian tube has demonstrated that TICs frequently coexisted with ovarian and peritoneal high-grade serous adenocarcinomas in the general population [8, 10]. Finally, analyses of TICs and ovarian carcinomas for p53 protein accumulation, *TP53* mutations, and chromosomal instability revealed similar genetic alterations in both tubal and ovarian lesions [8, 10, 11]. Indeed, these key findings provide evidence for designating TICs as preceding lesions of high-grade serous cancers. Nonetheless, previous reports on the association between fallopian tube lesions and ovarian and peritoneal cancers are from limited institutions in North America, and they focus primarily on serous carcinogenesis and the involvement of *TP53* gene alterations.

In the current study, we examined the coexistence of mucosal carcinoma of the fallopian tube among Japanese cases of ovarian and peritoneal cancer. The distribution of ovarian carcinoma cases according to their histological subtypes is different between Japan and Western countries. In Japan, the incidence of clear cell adenocarcinoma is much higher [19–21]. Consequently, we were able to include not only serous adenocarcinomas but also a large number of clear cell adenocarcinoma cases in this study. Our main objective was to assess whether the coexistence of mucosal carcinoma of the fallopian tube is a specific event in p53-positive high-grade serous carcinoma cases. In this report, we refrain from using the term "tubal intraepithelial carcinoma" (TIC) because it is now used widely as a term representing an early cancer that develops to form pelvic high-grade serous carcinoma, and some researchers emphasize p53 positivity as its key feature [7]. Instead, we use the term "mucosal carcinoma of the fallopian tube" to represent all histologically malignant tubal lesions that show intraepithelial growth, regardless of their immunophenotype.

Materials and methods

Case selection

We prospectively analyzed cases diagnosed as ovarian carcinoma or peritoneal serous carcinoma in four major hospitals in Tokyo, Japan (the University of Tokyo Hospital, Toranomon Hospital, Mitsui Memorial Hospital, and Teikyo University Hospital) between 2007 and 2009. The definitions of peritoneal and ovarian carcinomas were based on criteria adapted from the International Federation of Gynecology and Obstetrics (FIGO) and the World Health Organization [22, 23]. Cases with predominantly peritoneal tumor and minimal ovarian surface or tubal involvement were classified as peritoneal carcinomas. The diagnosis of ovarian carcinoma was confirmed when the bulk of the neoplasm was identified in the parenchyma of the ovary. Histological classification of the ovarian and peritoneal carcinomas was based on the most recent criteria of the World Health Organization [23]. Ovarian carcinomas diagnosed as serous adenocarcinomas were subcategorized as either low- or high-grade, according to a two-tier grading system (adapted from the MD Anderson Cancer Center grading system) [24]. Tumor staging was performed in accordance with the standards of FIGO, based on clinical information and pathological findings.

Section preparation and examination of resected specimens

For salpingo-oophorectomy specimens, we attempted to submit the fallopian tube, including the fimbria, in toto. The fallopian tubes were sectioned serially, approximately every 3 mm. The histological diagnosis of mucosal (in situ) carcinoma of the fallopian tube was based solely on morphology. Mucosal carcinoma was characterized by replacement of the normal tubal epithelium by malignant glandular epithelial cells with pleomorphic nuclei [23]. Stratification, loss of epithelial polarity, and lack of stromal invasion are other features of mucosal carcinoma of the fallopian tube. When peritoneal dissemination was sampled and submitted separately to the Department of Pathology, we evaluated its representative sections. The presence or absence of peritoneal dissemination was recorded in all the cases.

Completeness of tubal sectioning

We graded the completeness of the in toto tubal sectioning using a four-tier system, as described in Table 1. Of the 71

Table 1 Grading of completeness of in toto sectioning of the fallopian tubes and case distribution

	Submitted adnexa	Tumor involvement	In toto sectioning	Cases (n=71)
A (perfect)	Bilateral	Ovary: unilateral/bilateral Peritoneal dissemination: +/–	Completely performed bilaterally	40
B (satisfactory)	Unilateral	Ovary: clinically unilateral Peritoneal dissemination: –	Completely performed unilaterally (affected side)	8
	Bilateral	Ovary: histologically unilateral Peritoneal dissemination: –	Completely performed unilaterally (affected side)	1
C (adequate)	Bilateral/ unilateral	Ovary: histologically or clinically unilateral Peritoneal dissemination: +	Completely performed unilaterally (affected side)	3
		Ovary: histologically or clinically bilateral Peritoneal dissemination: +/–	Completely performed unilaterally (ipsilateral to the dominant ovarian mass)	3
D (inadequate)	Bilateral/ unilateral	Ovary: unilateral/bilateral Peritoneal dissemination: +/–	Incompletely performed in the tube ipsilateral to the dominant ovarian mass	16

MCFT mucosal carcinoma of the fallopian tube

ovarian and peritoneal cancer cases retrieved, we were able to perform appropriate sectioning in 55 cases (Grades A to C). As for peritoneal cancer cases, sectioning was considered appropriate only when bilateral fallopian tubes were perfectly sectioned. Three peritoneal serous adenocarcinoma cases were classified in the Grade A category. Reasons for incomplete sectioning (Grade D) included an unidentifiable fallopian tube due to replacement by tumor and inadequate sections made in the initial settings. Further clinicopathological analyses including a survey for mucosal carcinoma of the fallopian tube were performed on cases classified as Grades A to C.

Clinical survey of patients with serous adenocarcinoma

We examined the medical records of 15 serous adenocarcinoma (12 ovarian and three peritoneal) patients and their demographics: data including age, tumor site, preoperative diagnosis, survival status, and follow-up period were obtained. None of the patients underwent preoperative chemotherapy or radiotherapy. The follow-up period was calculated from the date of surgery to the date of death or last clinical evaluation. The mean follow-up interval was 11.9 months (range, 1-33). Medical records of non-serous adenocarcinoma patients were not investigated in this study.

Immunohistochemistry

Tissue samples were fixed in formalin and embedded in paraffin. For the serous adenocarcinoma cases, sections (4 μm) were cut from paraffin-embedded blocks containing ovarian or peritoneal tumor tissue and mucosal carcinoma of the fallopian tube, when present. Immunohistochemistry was performed with the following antibodies: mouse monoclonal anti-p53 antibody (1:100, Clone DO-7, Novocastra Laboratories, Newcastle Upon Tyne, UK), mouse monoclonal anti-Ki67 antibody (1:100, Clone MIB-1, Dako, Glostrup, Denmark), and mouse monoclonal anti-Wilms' tumor 1 (WT-1) protein (1:25, Clone 6F-H2, Dako). Immunohistochemical staining was performed according to standard techniques using a Ventana Benchmark® XT autostainer (Ventana Medical Systems Inc, Tucson, AZ, USA). Appropriate controls were included. p53 immunoreactivity was classified as completely negative (CN) when no cells showed any positive nuclear immunoreactivity, negative (N) when nuclear immunoreactivity was observed in <10% of cells, and positive (P) if ≥10% of cells showed strong nuclear immunoreactivity [25]. The percentage of cells with positive Ki-67 nuclear staining was interpreted as the proliferation index (MIB-1 index) for each lesion. MIB-1 index was quantified by counting at least 200 cells in the most immunoreactive area in each sample. As for minute lesions that consisted of less than 200 cells, all the cells were subjected to analysis. WT-1 immunoreactivity was assessed based on nuclear staining, and its intensity was classified subjectively as weak or strong. WT-1 immunoreactivity was scored as follows: 0 (totally negative or <10% of cells strongly/weakly positive), 1+ (≥10% of cells weakly positive and/or 10–50% of cells strongly positive), or 2+ (>50% of cells strongly positive). Additionally, the immunoreactivity of benign epithelium on the same sections, but away from mucosal carcinoma of the fallopian tube, was assessed with all three antibodies.

Examination of fallopian tubes for p53 signatures

To clarify the incidence of benign epithelium showing linear p53 immunopositivity (p53 signature) in the background tubal mucosa of serous adenocarcinoma cases and non-serous adenocarcinoma cases, we performed immunohistochemistry

for p53 in all the fallopian tube tissues sectioned in all of the serous adenocarcinoma cases (n=15) and in 15 cases of clear cell adenocarcinoma chosen as a control group. We made the diagnosis of p53 signature when greater than 75% of benign-looking tubal epithelial cells showed strong immunoreactivity for p53 in a linear manner, exceeding 12 cells in length, in accordance with a previous report [26].

Statistical analysis

Statistical analysis was performed using the χ^2 test. Statistical analyses were performed with StatView 5.0 software (SAS Institute, Cary, NC, USA), and $P<0.05$ was considered statistically significant.

Results

Ovarian and peritoneal carcinoma case distribution and presence of mucosal carcinoma of the fallopian tube

The distribution of the ovarian and peritoneal carcinoma cases and frequency of coexisting mucosal carcinoma of the fallopian tube are summarized in Table 2. Of the 55 cases properly examined for tubal lesions, three were peritoneal high-grade serous carcinoma cases and 52 were ovarian carcinoma cases. Histologically, our series consisted of 15 serous adenocarcinomas (14 high-grade serous adenocarcinomas and one low-grade serous adenocarcinoma), 23 clear cell adenocarcinomas, nine endometrioid adenocarcinomas, two mucinous adenocarcinomas, one mucinous borderline tumor with intraepithelial carcinoma, four mixed epithelial carcinomas, and one undifferentiated carcinoma. Perfect sectioning of the fallopian tubes (Grade A) was performed in 13/15 serous adenocarcinoma cases, and in 27/40 non-serous adenocarcinoma cases (P=0.155). Mucosal carcinoma of the fallopian tube was present only in the serous adenocarcinoma cases (7/15) and not in the non-serous adenocarcinoma cases (0/40; P=0.0001). We observed coexisting mucosal carcinoma of the fallopian tube in five ovarian high-grade serous adenocarcinoma cases, one ovarian low-grade serous adenocarcinoma case, and one peritoneal serous adenocarcinoma case. Perfect sectioning of the fallopian tubes (Grade A) was performed in all seven serous adenocarcinoma cases that had coexisting tubal lesions. Of the eight serous adenocarcinomas without coexisting tubal carcinoma, six were in the Grade A (perfect) sectioning category and two were in the Grade C (adequate) sectioning category. Statistically, grade of sectioning was not significantly different between serous adenocarcinoma cases with coexisting tubal lesions and those without (P=0.155).

Clinicopathological features of serous adenocarcinoma patients

Since early tubal carcinomas were associated only with ovarian/peritoneal serous adenocarcinomas, we specifically examined medical records of serous adenocarcinoma cases. The clinicopathological features including the immunophenotypes of 15 serous adenocarcinomas are summarized in Table 3. Cases 1–7 are cases with mucosal carcinomas of the fallopian tube, and cases 8–15 are those without. Histologically, all of the serous carcinomas except for case 1 were high-grade serous adenocarcinomas.

In case 1, the ovarian tumor showed features of low-grade serous adenocarcinoma, such as mild nuclear atypia, low mitotic activity (7 per 10 HPFs), coexistence of serous borderline (atypical proliferative) tumor component, and p53-negative (N) immunophenotype (Fig. 1). Its predominant architectural pattern was glandular and papillary pattern. A solid component was present, but focal.

In all ovarian serous adenocarcinoma cases with mucosal carcinomas of the fallopian tube, coexisting tubal lesions were found in the fimbriae ipsilateral to the dominant ovarian tumor. Mucosal carcinomas of the fallopian tube were multifocal in cases 1 and 2. In case 1, another mucosal carcinoma was found in non-fimbriated tubal mucosa ipsilateral to the dominant ovarian tumor. In case 2, ovarian carcinoma showed bilateral involvement, and minute mucosal carcinoma of the fallopian tube was also found in the fimbria contralateral to the dominant ovarian mass. With regard to patient age, tumor stage, and survival, we found no obvious difference between cases with and without mucosal carcinoma of the fallopian tube.

Histologically, in cases 2–4, the mucosal carcinomas of the fallopian tube in the ipsilateral side of the dominant

Table 2 Coexistence of mucosal carcinoma of the fallopian tube in ovarian and peritoneal cancer cases

Histology	Serous (n=15)	Non-serous (n=40)			
		Clear cell	Endometrioid	Mucinous	Others
Number of cases	15	23	9	3	5
Peritoneal dissemination (+)	13	7	0	0	1
Mucosal carcinoma of the fallopian tube (+)	7	0	0	0	0

Table 3 Clinicopathological and immunohistochemical features of serous adenocarcinoma cases

Case	Diagnosis	Age	Histological grade	Stage	Survival	PD	Sig	MCFT	p53 status	WT-1 status	MIB-1 index
1	OC	46	Low	III	NED (20 months)	+	−	+	N/N/N[a]	1+/2+/2+[a]	18/9/1[a]
2	OC	38	High	III	DOD (7 months)	+	−	+	P/P/N[a]	−/−/2+[a]	76/72/2[a]
3	OC	48	High	III	NED (2 months)	+	−	+	N/N/N[a]	2+/2+/2+[a]	71/54/1[a]
4	OC	46	High	III	AWD (15 months)	+	−	+	CN/CN/N[a]	2+/2+/1+[a]	56/55/1[a]
5	OC	47	High	III	NED (4 months)	+	−	+	CN/CN/N[a]	2+/2+/1+[a]	76/40/1[a]
6	OC	57	High	III	AWD (3 months)	+	+	+	P/P/N[a]	1+/2+/2+[a]	34/14/3[a]
7	PC	66	High	III	AWD (1 months)	+	+	+	P/P/N[a]	1+/2+/2+[a]	75/29/0[a]
8	OC	55	High	III	NED (19 months)	−	−	−	P[b]	1+[b]	46[b]
9	OC	59	High	I	NED (17 months)	−	−	−	P[b]	2+[b]	51[b]
10	OC	49	High	III	NED (15 months)	+	−	−	P[b]	2+[b]	44[b]
11	OC	35	High	IV	AWD (8 months)	+	−	−	P[b]	2+[b]	11[b]
12	OC	58	High	III	NED (9 months)	+	−	−	P[b]	2+[b]	42[b]
13	OC	38	High	III	NED (7 months)	+	+	−	N[b]	1+[b]	49[b]
14	PC	49	High	III	NED (18 months)	+	+	−	CN[b,c]	2+[b]	47[b]
15	PC	66	High	IV	AWD (33 months)	+	−	−	CN[b]	2+[b]	78[b]

PD peritoneal dissemination, *Sig* p53 signature, *MCFT* mucosal carcinoma of the fallopian tube, *WT-1* Wilms' tumor 1, *IT* invasive (ovarian or peritoneal) tumor, *BTE* benign tubal epithelium, *OC* ovarian carcinoma, *PC* peritoneal carcinoma, *NED* no evidence of disease, *AWD* alive with disease, *DOD* died of disease, *CN* completely negative, *N* negative, *P* positive

[a] IT/MCFT/BTE

[b] IT

[c] Completely negative except for one tubal lesion showing diffuse p53 positivity

ovarian tumor were in situ lesions by themselves, and no invasive carcinoma was found in continuity with them. In cases 1, 5, and 7, invasive tubal carcinoma was found in continuity or adjacent to the in situ lesions. Histology of the mucosal carcinoma of the fallopian tube was similar to that of the coexisting dominant invasive carcinoma mass in the ovary or peritoneum.

In case 1, the tubal lesion also had low-grade morphological features (Fig. 2). Uniform tumor cells with mild nuclear atypia replaced the tubal mucosa, and they displayed a prominent papillary growth pattern. Its histology was quite similar to that of a typical ovarian serous borderline tumor. Mucosal carcinomas of the fallopian tube in cases 2–7 were composed of tumor cells with marked nuclear atypia (Fig. 3). The presence of prominent nucleoli and frequent mitotic activity were also observed. In cases 3-7, mild to moderate inflammatory cell infiltration was observed in the stroma beneath the mucosal carcinomas of the fallopian tube. In some of these cases, there were histologically obvious cancer implantations in nearby tubal mucosa that were surrounded by desmoplastic stroma.

Immunohistochemical features of serous adenocarcinoma cases

Immunohistochemically, mucosal carcinomas of the fallopian tube that coexisted with ovarian/peritoneal serous adenocarcinomas showed higher MIB-1 index, compared with the benign fallopian tube epithelium (Figs. 2b and 3f). In all seven cases with coexisting mucosal carcinoma of the fallopian tube, both tubal lesions and invasive ovarian/peritoneal carcinomas showed similar immunophenotypes for p53 and WT-1. In case 1, the immunophenotype was only assessable in one of two coexisting mucosal carcinomas of the fallopian tube because the other tubal lesion disappeared in sections for immunohistochemistry. In case 2, two mucosal carcinomas of the fallopian tube showed similar immunophenotypes. Surprisingly, diffuse nuclear staining for p53 protein was observed only in three cases of ovarian/peritoneal carcinomas with coexisting tubal carcinomas (cases 2, 6, and 7; Fig. 3d). In the rest four cases, both invasive ovarian cancer and coexisting tubal carcinoma showed negative (either CN, completely negative; or N, negative) immunoreactivity for p53. Among them, cases 4 and 5 revealed completely negative (CN) immunophenotype for p53, and cases 1 and 3 showed negative (N) immunoreactivity (i.e., only scattered positive cells) for p53 (Figs. 1d and 2a).

Among eight ovarian and peritoneal serous carcinomas that had no coexisting mucosal carcinoma of the fallopian tube, five cases showed positive immunoreactivity for p53, one case revealed p53-completely negative (CN) immunophenotype, and one case was p53-negative (N). However, one remaining case (case 14) revealed an exceptional p53 immunophenotype. Case 14 was diagnosed as peritoneal high-grade serous adenocarcinoma. Along with many

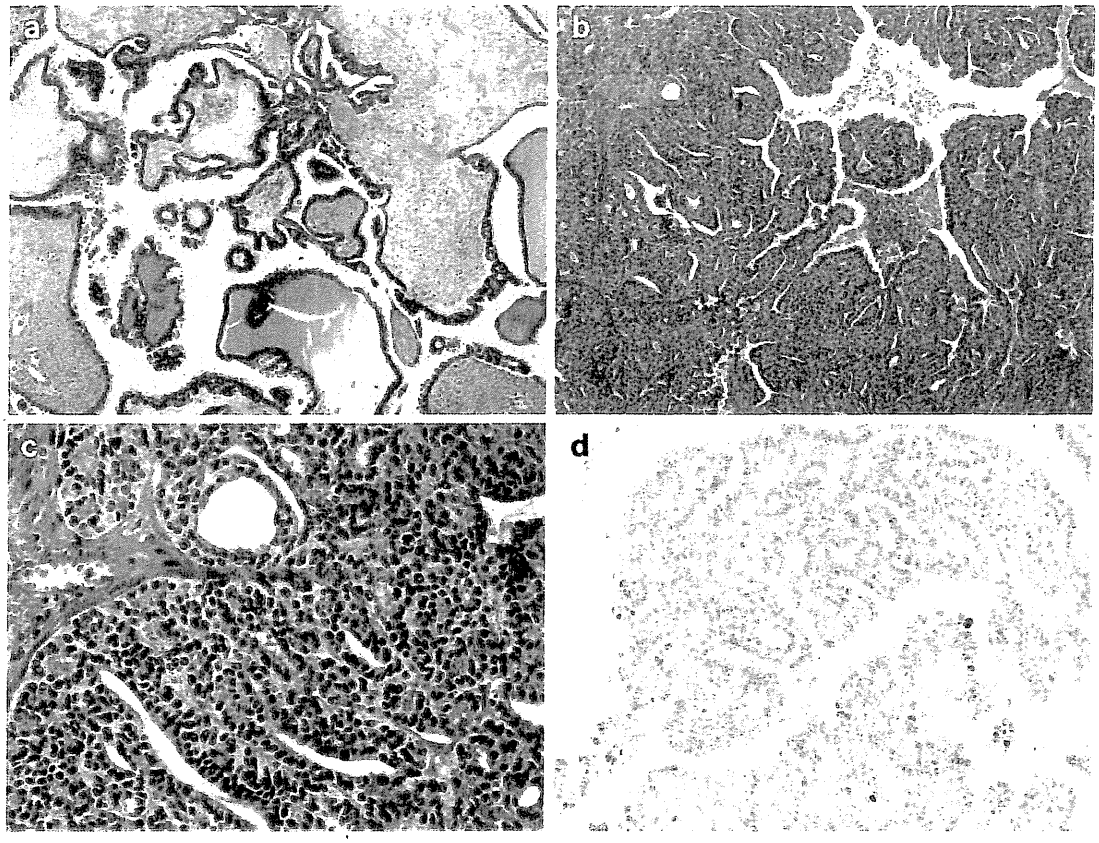

Fig. 1 Histology of ovarian tumor in case 1. **a** Serous borderline tumor component that coexisted with low-grade serous adenocarcinoma. **b** Majority of the ovarian mass was composed of low-grade serous adenocarcinoma showing papillary and glandular patterns of growth. **c** High-power view of the low-grade serous adenocarcinoma. Tumor cells are monotonous and their atypia is mild. **d** Low-grade serous adenocarcinoma showing only scattered immunoreactivity for p53

tumor foci in the omentum (Fig. 4a), we observed superficial involvement of bilateral ovaries (Fig. 4b) and a round discrete tumor nest in the submucosal stroma of the left tube (Fig. 4c). Although these tumor foci (omental, ovarian, and tubal) revealed similar morphological features, the p53 immunophenotype was significantly different between the omental/ovarian carcinoma and the left tubal carcinoma. After immunostaining all the slides that contained carcinoma, we found that all omental and ovarian carcinoma foci were completely negative (CN) for p53 (Fig. 4a, b) and that the left tubal carcinoma focus was diffusely positive for p53 (Fig. 4c). We then made serial sections of the left tubal lesion to examine whether mucosal carcinoma was in adjacent tubal mucosa. Deeper sections revealed tumor exposure in the tubal mucosal (Fig. 4d), but no in situ carcinoma component was identified.

p53 signature in the background tubal mucosa of serous and clear cell adenocarcinoma cases

The p53 signature was present in four of 15 cases of serous adenocarcinoma (Table 3). Of the cases with p53 signatures, two (cases 6 and 7) had coexisting mucosal carcinoma of the fallopian tube. Among the control group of clear cell adenocarcinoma cases, p53 signatures were found in seven of 15 cases (Fig. 5). The p53 signatures were often multifocal and, in some cases, bilateral. Of the 17 p53 signatures (five in serous adenocarcinoma cases and 12 in clear cell adenocarcinoma cases) detected in our series, 14 were located in the non-fimbriated tubal mucosa, and only three were in the fimbriated ends. The MIB-1 indices of the p53 signatures were very low, mostly below 5%, and no increase was observed in comparison with the index of the adjacent tubal mucosa.

Discussion

A newly introduced theory that designates the origin of ovarian cancer to the tubal epithelium has attracted significant attention. The theory is expected to explain, at least to some extent, the ovarian carcinogenesis that had for the most part been a mystery. However, it should be noted that only a few studies have assessed the association